

# Evidence for a novel cranial thermoregulatory pathway in thalattosuchian crocodylomorphs (#81259)

1

First submission

## Guidance from your Editor

Please submit by **27 Jan 2023** for the benefit of the authors (and your token reward) .



### Structure and Criteria

Please read the 'Structure and Criteria' page for general guidance.



### Raw data check

Review the raw data.



### Image check

Check that figures and images have not been inappropriately manipulated.

Privacy reminder: If uploading an annotated PDF, remove identifiable information to remain anonymous.

## Files

Download and review all files from the [materials page](#).

16 Figure file(s)

1 Table file(s)




# Structure and Criteria

---

## Structure your review

The review form is divided into 5 sections. Please consider these when composing your review:

1. BASIC REPORTING
2. EXPERIMENTAL DESIGN
3. VALIDITY OF THE FINDINGS
4. General comments
5. Confidential notes to the editor






 You can also annotate this PDF and upload it as part of your review

When ready [submit online](#).





## Editorial Criteria

Use these criteria points to structure your review. The full detailed editorial criteria is on your [guidance page](#).




### BASIC REPORTING

-  Clear, unambiguous, professional English language used throughout.
-  Intro & background to show context. Literature well referenced & relevant.
-  Structure conforms to [Peerj standards](#), discipline norm, or improved for clarity.
-  Figures are relevant, high quality, well labelled & described.
-  Raw data supplied (see [Peerj policy](#)).

### EXPERIMENTAL DESIGN

-  Original primary research within [Scope of the journal](#).
-  Research question well defined, relevant & meaningful. It is stated how the research fills an identified knowledge gap.
-  Rigorous investigation performed to a high technical & ethical standard.
-  Methods described with sufficient detail & information to replicate.

### VALIDITY OF THE FINDINGS

-  Impact and novelty not assessed. *Meaningful* replication encouraged where rationale & benefit to literature is clearly stated.
-  All underlying data have been provided; they are robust, statistically sound, & controlled.
-  Conclusions are well stated, linked to original research question & limited to supporting results.



The best reviewers use these techniques

## Tip

## Example

**Support criticisms with evidence from the text or from other sources**

*Smith et al (J of Methodology, 2005, V3, pp 123) have shown that the analysis you use in Lines 241-250 is not the most appropriate for this situation. Please explain why you used this method.*

**Give specific suggestions on how to improve the manuscript**

*Your introduction needs more detail. I suggest that you improve the description at lines 57- 86 to provide more justification for your study (specifically, you should expand upon the knowledge gap being filled).*

**Comment on language and grammar issues**

*The English language should be improved to ensure that an international audience can clearly understand your text. Some examples where the language could be improved include lines 23, 77, 121, 128 - the current phrasing makes comprehension difficult. I suggest you have a colleague who is proficient in English and familiar with the subject matter review your manuscript, or contact a professional editing service.*

**Organize by importance of the issues, and number your points**

- 1. Your most important issue*
- 2. The next most important item*
- 3. ...*
- 4. The least important points*

**Please provide constructive criticism, and avoid personal opinions**

*I thank you for providing the raw data, however your supplemental files need more descriptive metadata identifiers to be useful to future readers. Although your results are compelling, the data analysis should be improved in the following ways: AA, BB, CC*

**Comment on strengths (as well as weaknesses) of the manuscript**

*I commend the authors for their extensive data set, compiled over many years of detailed fieldwork. In addition, the manuscript is clearly written in professional, unambiguous language. If there is a weakness, it is in the statistical analysis (as I have noted above) which should be improved upon before Acceptance.*

# Evidence for a novel cranial thermoregulatory pathway in thalattosuchian crocodylomorphs

Mark T Young <sup>Corresp., 1, 2</sup>, Charlotte I W Bowman <sup>1</sup>, Arthur Erb <sup>1</sup>, Julia A Schwab <sup>1, 3</sup>, Lawrence M Witmer <sup>4</sup>, Yanina Herrera <sup>5</sup>, Stephen L Brusatte <sup>1</sup>

<sup>1</sup> School of GeoSciences, University of Edinburgh, Edinburgh, United Kingdom

<sup>2</sup> LWL-Museum für Naturkunde, Münster, Germany

<sup>3</sup> Department of Earth and Environmental Sciences, University of Manchester, Manchester, United Kingdom

<sup>4</sup> Department of Biomedical Sciences, Ohio University, Athens, Ohio, United States

<sup>5</sup> Museo de La Plata, Facultad de Ciencias Naturales y Museo, Universidad Nacional de La Plata, La Plata, Argentina

Corresponding Author: Mark T Young

Email address: marktyoung1984@gmail.com

Thalattosuchian crocodylomorphs were a diverse clade that lived from the Early Jurassic to the Early Cretaceous. The subclade Metriorhynchoidea underwent a remarkable transition, evolving from semi-aquatic ambush predators into fully aquatic forms living in the open oceans. Thalattosuchians share a peculiar palatal morphology with semi-aquatic and aquatic fossil cetaceans: paired anteroposteriorly aligned grooves along the palatal surface of the bony secondary palate. In extant cetaceans, these grooves are continuous with the greater palatine artery foramina, arteries that supply their oral thermoregulatory structures. Herein, we investigate the origins of thalattosuchian palatal grooves by examining CT scans of six thalattosuchian species (one teleosauroid, two early-diverging metriorhynchoidea and three metriorhynchids), and CT scans of eleven extant crocodylian species. All thalattosuchians had paired osseous canals, enclosed by the palatines, that connect the nasal cavity to the oral cavity. These osseous canals open into the oral cavity via foramina at the posterior terminus of the palatal grooves. Extant crocodylians lack both the external grooves and the internal canals. We posit that in thalattosuchians these novel palatal canals transmitted hypertrophied medial nasal vessels (artery and vein), creating a novel heat exchange pathway connecting the palatal vascular plexus to the endocranial region. Given the general hypertrophy of thalattosuchian cephalic vasculature, and their increased blood flow and volume, thalattosuchians would have required a more extensive suite of thermoregulatory pathways to maintain stable temperatures for their neurosensory tissues.

1 **Evidence for a novel cranial thermoregulatory pathway in**  
2 **thalattosuchian crocodylomorphs**

3

4 Mark T. Young <sup>1,2,\*</sup>, Charlotte I. W. Bowman <sup>1</sup>, Arthur Erb <sup>1</sup>, Julia A. Schwab <sup>1,3</sup>, Lawrence M.  
5 Witmer <sup>4</sup>, Yanina Herrera <sup>5</sup>, Stephen L. Brusatte <sup>1</sup>

6

7 <sup>1</sup> School of GeoSciences, Grant Institute, University of Edinburgh, James Hutton Road,  
8 Edinburgh, EH9 3FE, UK.

9 <sup>2</sup> LWL-Museum für Naturkunde, Sentruper Straße 285, 48161 Münster, Germany.

10 <sup>3</sup> Department of Earth and Environmental Sciences, The University of Manchester, Williamson  
11 Building, Oxford Road, Manchester M13 9PL, UK.

12 <sup>4</sup> Department of Biomedical Sciences, Heritage College of Osteopathic Medicine, Ohio  
13 University, Athens, Ohio, USA.

14 <sup>5</sup> Consejo Nacional de Investigaciones Científicas y Técnicas, División Paleontología  
15 Vertebrados, Museo de La Plata, Facultad de Ciencias Naturales y Museo, Universidad Nacional  
16 de La Plata, La Plata, Buenos Aires, Argentina.

17

18 Corresponding author: Mark T. Young

19 Email address: mark.young@ed.ac.uk

20

21 Keywords: Crocodylomorpha, Metriorhynchidae, Thalattosuchia, Thermoregulation, Vasculature

22



## 24 **ABSTRACT**

25 Thalattosuchian crocodylomorphs were a diverse clade that lived from the Early Jurassic to the  
26 Early Cretaceous. The subclade Metriorhynchoidea underwent a remarkable transition, evolving  
27 from semi-aquatic ambush predators into fully aquatic forms living in the open oceans.  
28 Thalattosuchians share a peculiar palatal morphology with semi-aquatic and aquatic fossil  
29 cetaceans: paired anteroposteriorly aligned grooves along the palatal surface of the bony  
30 secondary palate. In extant cetaceans, these grooves are continuous with the greater palatine  
31 artery foramina, arteries that supply their oral thermoregulatory structures. Herein, we investigate  
32 the origins of thalattosuchian palatal grooves by examining CT scans of six thalattosuchian  
33 species (one teleosauroid, two early-diverging metriorhynchoids and three metriorhynchids), and  
34 CT scans of eleven extant crocodylian species. All thalattosuchians had paired osseous canals,  
35 enclosed by the palatines, that connect the nasal cavity to the oral cavity. These osseous canals  
36 open into the oral cavity via foramina at the posterior terminus of the palatal grooves. Extant  
37 crocodylians lack both the external grooves and the internal canals. We posit that in  
38 thalattosuchians these novel palatal canals transmitted hypertrophied medial nasal vessels (artery  
39 and vein), creating a novel heat exchange pathway connecting the palatal vascular plexus to the  
40 endocranial region. Given the general hypertrophy of thalattosuchian cephalic vasculature, and  
41 their increased blood flow and volume, thalattosuchians would have required a more extensive  
42 suite of thermoregulatory pathways to maintain stable temperatures for their neurosensory  
43 tissues.

44

## 45 **INTRODUCTION**

46 Thalattosuchian crocodylomorphs underwent a major evolutionary transition during the Jurassic,  
47 evolving from semi-aquatic nearshore predators to fully aquatic forms which lived in the open  
48 oceans (Fraas, 1902; Andrews, 1913; Buffetaut, 1982; Young *et al.*, 2010; Wilberg, 2015; Ősi *et*  
49 *al.*, 2018; Schwab *et al.*, 2020). Thalattosuchia is composed of two subgroups: Teleosauroidea,  
50 which evolved a diverse range of semi-aquatic morphologies but never made the transition to  
51 being fully aquatic (Buffetaut, 1982; Johnson *et al.*, 2020); and Metriorhynchoidea, where the  
52 transition to life in the open ocean did occur (Fraas, 1902; Young *et al.* 2010; Wilberg 2015; Ősi  
53 *et al.*, 2018). Within Metriorhynchoidea, the fully aquatic subgroup Metriorhynchidae evolved a  
54 wide range of pelagic adaptations, including hydrofoil-like forelimbs, a hypocercal tail, loss of  
55 bony armour (osteoderms), and an osteoporotic-like lightening of the skull, femora and ribs (e.g.,  
56 Fraas, 1902; Andrews, 1913; Hua & Buffr nil, 1996; Young *et al.*, 2010). Metriorhynchids are  
57 also known to have had hypertrophied salt exocrine glands (Fern ndez & Gasparini, 2000, 2008;  
58 Fern ndez & Herrera, 2009; Herrera *et al.*, 2013; Cowgill *et al.*, 2022a) and smooth scaleless  
59 skin (Spindler *et al.*, 2021). They possibly also evolved viviparity (see Young *et al.*, 2010;  
60 Herrera *et al.*, 2017) and a poorly homeothermic form of endothermy (S on *et al.*, 2020).

61       Recently, computed tomography (CT) has been used to analyse the internal anatomy of  
62 thalattosuchian skulls, investigating their brains, sinuses, vasculature, salt glands and bony  
63 labyrinths (see Fern ndez & Herrera, 2009; Fern ndez *et al.*, 2011; Herrera *et al.*, 2013, 2018;  
64 Brusatte *et al.*, 2016; Pierce *et al.*, 2017; Schwab *et al.*, 2020, 2021; Bowman *et al.*, 2022;  
65 Cowgill *et al.*, 2022a, 2022b; Wilberg *et al.*, 2022). Thus, we are now beginning to get an  
66 unparalleled insight into the neurosensory and internal rostral soft-tissue anatomy of  
67 thalattosuchians, as well as the extensive changes that occurred within their crania as this group  
68 transitioned from being semi-aquatic to being fully aquatic.



69 One rostral structure that has not been investigated are the palatal grooves (sometimes  
70 also referred to as maxillo-palatine grooves, palatal canals, or anteroposterior sulci). All known  
71 thalattosuchians have paired anteroposteriorly aligned grooves on the roof of the oral cavity,  
72 present on the palatal surface of the palatines and maxillae (Fig. 1; Andrews, 1913; Parrilla-Bel  
73 *et al.*, 2013; Foffa & Young 2014; Johnson *et al.*, 2019, 2020; Aiglstorfer *et al.*, 2020; Young *et*  
74 *al.*, 2020a, 2021). What formed the palatal grooves is unknown. Given that this feature is  
75 ubiquitous within Thalattosuchia, but absent in other crocodylomorphs, it is possible that these  
76 grooves are linked to the land to sea transition that thalattosuchians underwent. To determine  
77 whether this is correct, here we investigate the palatal grooves in CT scans of six thalattosuchian  
78 species. We discovered that the posterior terminus of the grooves (on the palatines) is continuous  
79 with ossified canals that connect the oral cavity to the nasal cavity. Given their location, we  
80 hypothesise that these canals primarily held vasculature, and that the medial nasal arteries and  
81 veins, which are present in virtually all extant diapsids (Porter & Witmer 2015, 2016; Porter *et*  
82 *al.*, 2016), took a novel course and were transmitted along the external grooves. This would have  
83 connected the palatal vascular plexus to the ethmoid vessels, creating a new heat exchange  
84 pathway that would have helped moderate brain and eye temperatures.

85

## 86 INSTITUTIONAL ABBREVIATIONS

87 **AMNH**, American Museum of Natural History, New York City, New York, USA; **CM**,  
88 Carnegie Museum of Natural History, Pittsburgh, Pennsylvania, USA; **FMNH**, Field Museum of  
89 Natural History, Chicago, Illinois, USA; **IRSNB**, Institut Royal des Sciences Naturelles de  
90 Bruxelles, Belgium; **IVPP**, Institute of Paleontology and Paleoanthropology, Beijing, China;  
91 **IWCMS**, Isle of Wight County Museums Services (Dinosaur Isle Museum and visitor attraction)

92 Sandown, United Kingdom; **MLP**, Museo de La Plata, La Plata, Argentina; **MM**, Minden  
93 Museum, Minden, Germany; **MNB**, National Museum of the Bahamas, Nassau, Bahamas;  
94 **MNHN**, Muséum national d'Histoire naturelle, Paris, France; **MTM**, Magyar  
95 Természettudományi Múzeum, Budapest, Hungary; **NMS**, National Museum of Scotland,  
96 Edinburgh, Scotland, UK; **NHMUK**, Natural History Museum, London, UK; **OUVC**, Ohio  
97 University, Vertebrate Collection, Athens, Ohio, USA; **TMM**, Texas Memorial Museum,  
98 University of Texas at Austin, Austin, Texas, USA; **UF**, University of Florida, Florida Museum  
99 of Natural History, Gainesville, Florida, USA; **USNM**, National Museum of Natural History,  
100 Washington DC, USA.

101

## 102 **MATERIALS & METHODS**

103 We made internal rostral reconstructions of six thalattosuchian skulls based on CT scans  
104 (see Table 1). Our sample includes the teleosauroid *Plagiophthalmosuchus gracilirostris*  
105 (NHMUK PV OR 33095); two early-diverging metriorhynchoids *Pelagosaurus typus* (NHMUK  
106 PV OR 32599) and *Eoneustes gaudryi* (NHMUK PV R 3263); and three metriorhynchids,  
107 *Thalattosuchus superciliosus* (NHMUK PV R 11999), *Cricosaurus araucanensis* (MLP 72-IV-  
108 7-1) and *Cricosaurus schroederi* (MM Pa1). Apart from *Pl. gracilirostris* and *Cri. araucanensis*,  
109 which have nearly complete rostra, all the thalattosuchian specimens are missing the anterior  
110 portion of the rostrum (comprising the premaxilla and the anterior end of the maxilla) but  
111 preserve the portions relevant to this study.

112 The fossils were segmented manually using Materialise Mimics Innovation Suite (version  
113 24.0, Materialize NV 2021) using the livewire tool. The palatal canals were identified in coronal  
114 view as circular or elliptical holes in the palatine bones that bud off the nasal cavity and form a

115 canal oriented anteroventrally which communicates ventrally with the oral cavity. To aid our  
116 understanding of palatal vasculature in extant crocodylians, we examined a CT scan of a skull of  
117 *Alligator mississippiensis* (OUVC 9757) where the arteries and veins had been injected with a  
118 barium-latex contrast medium prior to CT scanning, which created a strong contrast between the  
119 vessels and surrounding tissues (see Porter *et al.*, 2016). The vessels were segmented as one  
120 mask by using the threshold segmentation tool on the full scan in Materialize Mimics. The  
121 palatal vessels and plexus were then removed from this first mask and segmented using the  
122 threshold tool in coronal view at every fifth slice. The 3D interpolate function was then used to  
123 fill in the gaps between these slices.

124 To compare the osteology of the crania, the thalattosuchians were compared to CT scans  
125 of 17 extant crocodylians from 11 species (Figs. 2C, 2D, and 3). We included two species of  
126 alligatorid, *Alligator mississippiensis* (OUVC 10606, OUVC 9761, OUVC 11415, TMM M-983,  
127 and USNM 211233) and *Caiman crocodilus* (FMNH 73711); seven species of crocodylid,  
128 *Crocodylus acutus* (FMNH 59071), *Cro. johnstoni* (TMM M-6807), *Cro. moreletii* (TMM M-  
129 4980), *Cro. porosus* (OUVC 10899), *Cro. rhombifer* (MNB AB50.071), *Mecistops cataphractus*  
130 (TMM M-3529), and *Osteolaemus tetraspis* (FMNH 98936); and two species of gavialid,  
131 *Gavialis gangeticus* (TMM M-5490 and UF herp 118998) and *Tomistoma schlegelii* (TMM M-  
132 6342 and USNM 211322). Our sample spanned the entire range of crocodylian snout shapes,  
133 from broad platyrostral to tubular longirostrine (see Figure 3). Finally, we included multiple  
134 specimens of *A. mississippiensis*, *G. gangeticus* and *To. schlegelii* to ascertain whether the  
135 presence of palatal grooves was impacted by ontogeny.

136

## 137 **Results**

138 All thalattosuchian skulls in our sample have paired osseous canals that are enclosed by  
139 the palatines (Figs. 4-9). These canals are oriented anteroventrally connecting the nasal cavity to  
140 the oral cavity (Figs. 4-9). They open into the oral cavity via paired foramina at the posterior  
141 terminus of the palatal grooves (best seen in *Pelagosaurus typus*, Fig. 1B). In the semi-aquatic  
142 thalattosuchians (i.e. the teleosauroid *Plagiophthalmosuchus* and the early-diverging  
143 metriorhynchoid *Pelagosaurus*), the canals are almost horizontal when seen in lateral view (Figs.  
144 4C and 5C) and converge at a shallow angle when seen in dorsal view (Figs. 4B and 5B). In  
145 contrast, *Eoneustes* and the fully aquatic metriorhynchids have palatal canals that noticeably  
146 angled anteroventrally when seen in lateral view (Figs. 6C, 7C, 8C, and 9C). The  
147 metriorhynchids also have canals that converge anteriorly at a greater angle (Figs. 7B, 8B, and  
148 9B).

149 The thalattosuchian skulls in our sample also had paired anteroposteriorly aligned  
150 parasagittal grooves on the palatal surface of the palatines and maxilla (= palatal grooves; Figs.  
151 1, 2A, and 2B). These grooves are a synapomorphy of Thalattosuchia, and are present in all  
152 examined teleosauroids and metriorhynchoids (e.g. Andrews, 1913; Parrilla-Bel *et al.*, 2013;  
153 Foffa & Young, 2014; Johnson *et al.*, 2019, 2020; Aiglstorfer *et al.*, 2020; Hua, 2020; Young *et*  
154 *al.*, 2020a, 2021; Figs. 1, 2A and 2B). In *Plagiophthalmosuchus* and *Pelagosaurus*, the grooves  
155 are close to the skull midline and remain parallel on the palatines and for most of the maxilla  
156 (diverging only in the anterior-most region of the maxilla) (see Andrews, 1913; Pierce & Benton,  
157 2006; Johnson *et al.*, 2019, 2020; Figs. 1A, 1B, and 2A). In metriorhynchids however, the  
158 grooves diverge at the anterior palatines, and on the maxilla the grooves become largely parallel  
159 but are much more widely separated than in non-metriorhynchid thalattosuchians (see Andrews,  
160 1913; Parrilla-Bel *et al.*, 2013; Foffa & Young, 2014; Young *et al.*, 2020a, 2021; Fig. 1). The

161 shift in morphology occurs gradually within Metriorhynchoidea, as the palatal grooves become  
162 more widely spaced relative to the maxillary midline in the early-diverging metriorhynchoids  
163 *Teleidosaurus*, *Opisuchus* and *Eoneustes*, being intermediate between *Pelagosaurus* and  
164 metriorhynchids (see Aiglstorfer *et al.*, 2020; Hua, 2020; NHMUK PV R 3263).

165 In contrast, all of the extant crocodylian skulls in our sample lacked the external palatal  
166 grooves (Figs. 2C, 2D, and 3) and the internal canals (Figs. 10 and 11). This was true for  
167 alligatorids (*Alligator mississippiensis* and *Caiman crocodilus*), crocodylids (*Crocodylus acutus*,  
168 *Cro. johnstoni*, *Cro. moreletii*, *Cro. porosus*, *Cro. rhombifer*, *Mecistops cataphractus*, and  
169 *Osteolaemus tetraspis*) and gavialids (*Gavialis gangeticus* and *Tomistoma schlegelii*). Moreover,  
170 the grooves and canals are not present in any of the different ontogenetic stages we examined,  
171 including the hatchling (Fig. 3A), juveniles (Figs. 3B, 3C, 3D, and 3J), subadults (Figs. 3F, 3L,  
172 3N, and 3P) and adults (Figs. 3E, 3K, 3M, 3O, and 3Q). Based on our sample of thalattosuchians  
173 and extant crocodylians we posit that the osseous palatal canals and the external grooves are  
174 linked. Both structures are continuous, and are only found to co-occur (i.e. skulls lacking palatal  
175 grooves also lack internal palatal canals, and skulls which have palatal grooves also have internal  
176 palatal canals).

177 Based on first-hand examination of extant crocodylian skulls, the grooves are also absent  
178 in the following specimens: the gavialids *Gavialis gangeticus* (NHMUK 1935-6-4-1, NHMUK  
179 1946-1-7-3, NHMUK 1996-7-7-4, NHMUK 2005-1601) and *Tomistoma schlegelii* (NHMUK  
180 1948-10-31-19); the crocodylids *Mecistops cataphractus* (NHMUK 64.4.4.1), *Osteolaemus*  
181 *tetraspis* (NHMUK 1961-3-20-8, NHMUK 1962-6-30-5, NMS Z.2013.175, NMS Z.2014.3),  
182 *Crocodylus acutus* (NHMUK 1975.997), *Cro. halli* (NHMUK 1886.5.20.1, NHMUK  
183 1886.5.20), *Cro. intermedius* (NMS Z.1945.42), *Cro. moreletii* (NHMUK 1861.4.14), *Cro.*

184 *niloticus* (NHMUK 1949-1-1-2, NHMUK 1959.1.8.55), *Cro. palustris* (NHMUK 1868.4.9.11,  
185 NMS Z.1945.43), *Cro. porosus* (NHMUK 1847.3.5.33, NHMUK 1929-2-225-3803, NHMUK  
186 1943-8-18-4, NHMUK 1947-3-5-33), *Cro. rhombifer* (NMS Z.2014.18.2), and *Cro. siamensis*  
187 (NHMUK 1921.4.1.168); and the alligatorids *Alligator mississippiensis* (NHMUK 68.2.12.6,  
188 NHMUK ZD 290, NHMUK ZD 1973-2-21-2, NHMUK ZD 1974-3010, NHMUK ZD 1975-  
189 1424, NHMUK ZD II-1-I), *Alligator sinensis* (NHMUK X184), *Caiman crocodilus* (NHMUK  
190 1898.9.26.1, NHMUK 1933.5.10.1), *Caiman latirostris* (NHMUK 2008-270, NHMUK  
191 86.10.4.2), *Melanosuchus niger* (NHMUK 1945-8-25-126), and *Paleosuchus trigonatus*  
192 (NHMUK 1868.10.8.1). Coupled with our CT analyses, this broader sampling of extant  
193 crocodylians shows that the longitudinal palatal grooves cannot be found in extant species.

194 In extinct taxa, the longitudinal grooves are absent on the maxilla and/or palatine, based  
195 on first-hand examination in: the atoposaurid *Theriosuchus pusillus* (NHMUK PV OR 48216);  
196 the goniopholidids *Anteophthalmosuchus hooleyi* (NHMUK PV R 3876; Ristevski *et al.*, 2018),  
197 *Anteophthalmosuchus epikrator* (IWCMS 2001.446, IWCMS 2005.127; Ristevski *et al.*, 2018),  
198 and *Eutretauranosuchus delfsi* (CM 8028; Pritchard *et al.*, 2013); the pholidosaurids  
199 *Pholidosaurus purbeckensis* (NHMUK PV R 3956, NHMUK PV R 36721) and *Terminonarus*  
200 *browni* (AMNH 5851); the early-diverging dyrosauroids *Elosuchus broinae* (MNHN.F SAM  
201 129; Meunier & Larsson, 2017) and *Elosuchus cherifensis* (MNHN.F MRS 340; Meunier &  
202 Larsson, 2017); the bernissartiid *Koumpiodontosuchus aprosdokiti* (IWCMS 2012.203-204;  
203 Sweetman *et al.*, 2015); the hylaeochampsid *Iharkutosuchus makadii* (MTM 2006.52.1; Ösi *et*  
204 *al.*, 2007); the early-diverging gavialoid *Eosuchus lerichei* (IRSNB-R-49; Delfino *et al.*, 2005);  
205 the crocodylids *Voay robustus* (NHMUK PV R 36684, NHMUK PV R 36685), *Brochuchus*  
206 *pigotti* (NHMUK PV R 7729) and *Crocodylus palaeindicus* (NHMUK PV OR 39795); and the


207 alligatoroid *Diplocynodon hantoniensis* (NHMUK PV OR 25166, NHMUK PV OR 30392; Rio  
208 *et al.*, 2020).

209 Based on information from the literature, the grooves are also absent in: the  
210 shartegosuchoid *Shartegosuchus asperapalatum* (Dollman *et al.*, 2018); the sphagesaurids  
211 *Caipirasuchus montealtensis* (Andrade & Bertini, 2008), *Sphagesaurus huenei* (Pol, 2003) and  
212 *Yacarerani boliviensis* (Novas *et al.*, 2009); the baurusuchids *Campinasuchus dinizi* (Carvalho *et*  
213 *al.*, 2011) and *Baurusuchus salgadoensis* (Carvalho *et al.*, 2005); the sebecians *Hamadasuchus*  
214 *rebouli* (Larsson & Sues, 2007), *Kaprosuchus saharicus* (Serenó & Larsson, 2009) and  
215 *Montealtosuchus arrudacamposi* (Carvalho *et al.*, 2007); the goniopholidids *Calsoyasuchus*  
216 *valliceps* (Tykoski *et al.*, 2002) and *Hulkepholis willetti* (Salisbury & Naish, 2011); the  
217 paluxysuchid *Paluxysuchus newmanni* (Adams, 2013); the pholidosaurids *Meridiosaurus*  
218 *vallisparadisi* (Fortier *et al.*, 2011) and *Oceanosuchus boecensis* (Hua *et al.*, 2007); the  
219 dyrosaurids *Anthracosuchus balrogus* (Hastings *et al.*, 2015), *Cerrejonisuchus improcerus*  
220 (Hastings *et al.*, 2010), *Dyrosaurus maghribensis* (Jouve *et al.*, 2006) and *Guarinisuchus munizi*  
221 (Barbosa *et al.*, 2008); the susisuchid *Isisfordia duncani* (Salisbury *et al.*, 2006); the bernissartiid  
222 *Bernissartia fagesii* (Martin *et al.*, 2020); the paralligatorids *Rugosuchus nonganensis* (Wu *et al.*,  
223 2001) and *Shamosuchus* spp. (Turner, 2015); the allodaposuchids *Allodaposuchus precedens*  
224 (Delfino *et al.*, 2008) and *Lohuecosuchus megadontos* (Narváez *et al.*, 2015); and the gavialoid  
225 *Hanyusuchus sinensis* (Iijima *et al.*, 2022).

226

## 227 **DISCUSSION**

### 228 **Palatal structures in Crocodylomorpha**

229 The presence of palatal grooves is one of the defining characteristics of Thalattosuchia  
230 (Andrews, 1913; Parrilla-Bel *et al.*, 2013; Foffa & Young, 2014; Johnson *et al.*, 2019, 2020;  
231 Aiglstorfer *et al.*, 2020; Young *et al.*, 2020a, 2021). As we note herein, these grooves are not  
232 found in extant crocodylians, irrespective of their ontogenetic stage. Given that no other  
233 mesoeucrocodylian taxon with a maxillopalatine secondary palate has been observed to have  
234 palatal grooves, we posit that they are synapomorphies of Thalattosuchia. This is in agreement  
235 with phylogenetic analyses that have found these features to be explicit thalattosuchian  
236 synapomorphies (e.g. Johnson *et al.*, 2020; Young *et al.*, 2020a, 2021). The only other  
237 crocodylomorph known to have prominent palatal foramina and depressions is the notosuchian  
238 *Simosuchus clarki*. Kley *et al.* (2010: 38, figures 3B, 8F) described paired palatal fossae on the  
239 anterior palatal rami of the maxilla, at the premaxilla-maxilla boundary. Within each deep fossa  
240 is a palatal foramen. However, given their anterior position and lack of palatal grooves we do not  
241 seem consider them to be homologous to the palatal canals found in thalattosuchians. In the same  
242 location, large foramina are also found in the allodaposuchid *Lohuecosuchus megadontos*,  
243 however there is no surrounding fossa (Narváez *et al.*, 2015). Interestingly, mid-way along the  
244 maxilla there are paired foramina close to the skull midline in *Lohuecosuchus megadontos*  
245 (Narváez *et al.*, 2015). However, these palatal foramina are not found in any other species of  
246 allodaposuchid (Narváez *et al.*, 2015: 25). 

247

#### 248 **Palatal grooves in aquatic mammals and oral vascularisation**

249 While no crocodylomorph clade shares the paired longitudinal palatal grooves seen in  
250 Thalattosuchia, curiously fossil and extant cetaceans do. A very similar morphology is present in  
251 the semi-aquatic remingtonocetid *Remingtonocetus harudiensis* (Bajpai *et al.*, 2011: figure 1.3),



252 the semi-aquatic protocetid *Aegyptocetus tarfa* (Bianucci & Gingerich, 2011: figure 3), and in  
253 fully aquatic forms, including the early-diverging mysticete *Aetiocetus weltoni* (Ekdale &  
254 Deméré, 2022: figure 2A), the early-diverging odontocetes *Simocetus rayi* (Fordyce, 2002: figure  
255 4) and *Echovenator sanderi* (Churchill *et al.*, 2016: figures 1F, 1G), and the beluga-like  
256 odontocete *Bohaskaia monodontoides* (Veléz-Juarbe & Pyenson, 2012: figure 3). The same  
257 morphology has also been described and figured for the extant gray whale (*Eschrichtus robustus*)  
258 and finback whale (*Balaenoptera physalus*) (see Ekdale *et al.*, 2015), and is also present in the  
259 humpback whale (*Megaptera novaeangliae*) (Fig. 12). There are four striking parallels between  
260 thalattosuchians and cetaceans: (1) the presence of anteroposteriorly aligned (longitudinal)  
261 grooves, present along most of the maxilla with their posterior terminus either on the palatines  
262 (as in thalattosuchians) or at the maxilla-palatine suture (cetaceans); (2) the longitudinal grooves  
263 have a large foramen at their posterior terminus; (3) in both clades the morphology is present in  
264 both semi-aquatic and fully aquatic forms; and (4) the grooves are closer to the skull midline in  
265 the semi-aquatic forms (see *Pelagosaurus* herein and *Remingtonocetus* in Bajpai *et al.*, 2011),  
266 whereas in the fully aquatic forms the grooves are much more widely spaced (see the  
267 metriorhynchids herein, and *Aetiocetus* in Ekdale & Deméré, 2022; *Simocetus* in Fordyce, 2002;  
268 *Echovenator* in Churchill *et al.*, 2016 and *Bohaskaia* in Veléz-Juarbe & Pyenson, 2012).  
269 Intermediate morphologies also appear in cetacean evolution, such as in *Aegyptocetus* (Bianucci  
270 & Gingerich, 2011).

271 In extant whales, the greater (or descending) palatine artery exits through the palatal  
272 foramen and continues anteriorly via the longitudinal groove/sulcus (Deméré *et al.*, 2008; Ekdale  
273 *et al.*, 2015). This has also been hypothesised for fossil cetaceans (e.g. Bajpai *et al.*, 2011; Veléz-  
274 Juarbe & Pyenson, 2012; Ekdale & Deméré, 2022). Although there has been a long discussion on

275 whether the greater palatine artery is associated with the evolution of baleen in mysticetes, this  
276 hypothesis seems to have been falsified (see Ekdale *et al.*, 2015; Ekdale & Deméré, 2022). Two  
277 further hypotheses have been suggested for the expansion of the palatine vasculature in  
278 cetaceans, positing that it is either a consequence of rostral elongation (Ichishima *et al.*, 2008) or  
279 for thermoregulation (Ekdale *et al.*, 2015). Ekdale *et al.* (2015: 699), however, noted that similar  
280 structures are not found in other mammals with elongate snouts (although the palatine foramina,  
281 and some form of palatal grooves, are). Within Crocodylomorpha there are numerous long-  
282 snouted groups, both extinct and extant, but none show evidence of palatal grooves. Moreover,  
283 among extant species long-snouted taxa do not have expanded rostral vasculature compared to  
284 broader snouted species (e.g. Bowman *et al.*, 2022).

285         Mysticetes have highly vascularised oral cavities, with the mouth being an important site  
286 for thermoregulation (e.g., Ford & Krause, 1992; Werth, 2007; Ford *et al.*, 2013; Ekdale *et al.*,  
287 2015). This is unsurprising given that mysticetes bulk filter feed, which involves the mouth being  
288 repeatedly exposed to (often cold) sea water. However, odontocetes seem to lack vascular  
289 adaptations for thermoregulation within the oral cavity (Werth, 2007). This is supported by the  
290 palatine foramen being greatly reduced, or almost closed, in extant delphinoid odontocetes  
291 (although the foramina are greatly enlarged in the fossil genus *Odobenocetops*, see de Muizon *et*  
292 *al.*, 2002), although the grooves are present in the killer whale (*Orcinus orca*) and Cuvier's  
293 beaked whale (*Ziphius cavirostris*) (Fig. 13). Werth (2007) suggested that for odontocetes there  
294 was either less need to prevent oral heat loss, or that other regions of the body were more  
295 important sites for thermoregulation.

296         During their land-to-sea transition, pinnipedimorphs (seals and their close fossil relatives)  
297 evolved a similar morphology (Fig. 14). In early-diverging forms such as *Enalioarctos*, the


298 palatal grooves originating from the palatine foramina are relatively short (Berta, 1991). During  
299 phocid ('true seals') evolution, however, the grooves became increasingly broader and more  
300 elongated (Dewaele *et al.*, 2018; Rule *et al.*, 2020; Koretsky & Rahmat, 2021).

301 Many other amniote groups have a venous plexus within the soft tissues of the palate. In  
302 birds, the palatal plexus and the rete ophthalmicum help maintain eye and brain temperature  
303 (Kilgore *et al.*, 1979, Midtgård 1983, 1984, Porter & Witmer 2016), while in extant crocodylians  
304 there is an extensive palatal plexus (Porter *et al.*, 2016). In extant archosaurs the palatal plexus is  
305 supplied by the palatine artery (Figs. 15 and 16); however, the palatine arteries travel through the  
306 soft tissue of the secondary palate (see Porter & Witmer 2016; Porter *et al.*, 2016), unlike in  
307 cetaceans where they pass through the bony palate. Moreover, in extant archosaurs the palatine  
308 arteries are situated laterally in the rostrum (see Fig. 15; Porter & Witmer 2016; Porter *et al.*,  
309 2016), not medially as in cetaceans. We propose an osteological correlate for the palatine vessels  
310 in thalattosuchians: the groove that originates at the anterior margin of the suborbital fenestra  
311 (Fig. 1: SOG). This groove is consistent with location of the palatine vessels in extant  
312 crocodylians (Porter *et al.*, 2016).

313 Based on the striking similarity between thalattosuchian palatal canal/groove system and  
314 those of cetaceans (particularly the fossil semi-aquatic and aquatic species), and the known  
315 routes and positions of extant crocodylian cranial vasculature, we hypothesise the following:

316 1. The thalattosuchian palatal canal/groove system transmitted the medial nasal vessels  
317 (artery and vein) or a novel branch thereof, and possibly also some of the rostral  
318 nerves. In all extant diapsids, the medial nasal vessels branch off from nasal vessels at  
319 the posterodorsal aspect of the nasal cavity. The medial nasal vessels then descend  
320 anteroventrally on either side of the median cartilaginous internasal septum to run on

321 the floor of the nasal cavity (e.g. Figs. 15 and 16; Porter & Witmer 2015, 2016; Porter  
322 *et al.*, 2016). Therefore, the paramedian/parasagittal position of the palatal  
323 canal/groove system in thalattosuchians is consistent with the medial nasal vessels.

- 324 2. Early in thalattosuchian evolution, the medial nasal vessels (or a ventral branch  
325 thereof) pierced the bony palate to emerge on to the roof of the oral cavity 
- 326 3. The medial nasal vessels that entered the oral cavity anastomosed with the palatal  
327 vascular plexus (which are supplied by the palatine vessels).
- 328 4. The large internal osseous canals represent a hypertrophy of the medial nasal vessels.
- 329 5. A novel heat exchange pathway was created by linking the palatal plexus to medial  
330 nasal vessels. In extant crocodylians, the medial nasal vessels communicate with the  
331 encephalic arteries and veins via the ethmoid vessels (Porter *et al.*, 2016). The palatal  
332 vascular plexus is a critical location of thermal exchange in extant crocodylians  
333 (Porter *et al.*, 2016). While the palatal plexus is not thought to have a substantial role  
334 in thermoregulation of the brain in extant crocodylians, based on our proposed  
335 vascular pathway, the palatal plexus ~~would~~ have moderated brain temperatures of  
336 thalattosuchians via the ethmoid vessels.

337

### 338 **Increased cephalic blood volume in Thalattosuchia**

339 A novel heat exchange pathway to help maintain brain and eye temperatures would have been  
340 greatly beneficial for Metriorhynchidae. Not only did metriorhynchids have an elevated  
341 metabolism (possibly a poorly homeothermic form of endothermy, see Séon *et al.*, 2020), but  
342 they had expanded cerebral hemispheres and orbits relative to extant crocodylians and other  
343 thalattosuchians (e.g. see Young *et al.*, 2010; Herrera *et al.*, 2018; Schwab *et al.*, 2021). An

344 obvious question is why would semi-aquatic thalattosuchians also have had a novel heat  
345 exchange pathway? One of the defining features of Thalattosuchia is the enlarged cerebral  
346 carotid foramina on the occipital surface of the cranium, being found in both semi-aquatic and  
347 fully aquatic species (Andrews, 1913; Pierce & Benton, 2006; Jouve, 2009; Pol & Gasparini,  
348 2009; Fernández *et al.*, 2011; Young *et al.*, 2012, 2013, 2020b; Herrera & Vennari, 2015;  
349 Brusatte *et al.*, 2016; Johnson *et al.*, 2020). Note, the cerebral carotid foramina become even  
350 larger in the clade *Zoneait* + Metriorhynchidae (Wilberg, 2015; Herrera *et al.*, 2018), while they  
351 become smaller in some freshwater teleosauroids (Herrera *et al.*, 2018). In mammals, larger  
352 encephalic arteries are associated with higher rates of blood flow, as flow (perfusion) is  
353 proportional to the radius of the arterial lumen raised to an exponent of approximately 2.5  
354 (Seymour *et al.*, 2019). In extant crocodylians, the cerebral carotid arteries supply blood to the  
355 brain, eyes, nasal cavities, and the rostral sinuses (Porter *et al.*, 2016). Therefore, it is possible  
356 that these vessels supplied a greater volume of blood to these regions in thalattosuchians  
357 compared to extant crocodylians.

358 Further, these enlarged foramina do not represent the full extent of vascular hypertrophy  
359 observed in thalattosuchian skulls. The cerebral carotid vessels enter the greatly enlarged  
360 pituitary fossa chamber, another thalattosuchian synapomorphy, which in extant crocodylians  
361 houses the cavernous venous sinus (Porter *et al.*, 2016) and was possibly hypertrophied in  
362 thalattosuchians. Exiting the anterior margin of the pituitary fossa chamber are two ossified  
363 canals thought to transmit the orbital arteries (Brusatte *et al.*, 2016), with these canals being  
364 almost as wide as the cerebral carotid canals (Brusatte *et al.*, 2016; Pierce *et al.*, 2017; Herrera *et*  
365 *al.*, 2018; Wilberg *et al.*, 2022). Within Crocodylomorpha, only thalattosuchians and the  
366 dyrosaurid *Rhabdognathus* (Erb & Turner, 2021) are known to have the orbital arteries contained

367 within ossified canals. Further, the midbrain and hindbrain of thalattosuchians are very poorly  
368 delineated in their endocasts due to the hypertrophy of the longitudinal and transverse dural  
369 venous sinuses, the latter being continuous with the hypertrophied stapedia canals (Wharton,  
370 2000; Fernández *et al.*, 2011; Brusatte *et al.*, 2016; Pierce *et al.*, 2017; Herrera *et al.*, 2018;  
371 Schwab *et al.*, 2021; Wilberg *et al.*, 2022). Collectively, this implies that thalattosuchians had  
372 increased encephalic blood volumes and potentially increased perfusion rates relative to extant  
373 crocodylians. As such, maintaining stable brain and eye temperatures may have required more  
374 extensive heat exchange mechanisms.

375         Unfortunately, we do not know the timing of these internal changes. All examined  
376 thalattosuchians show the same suite of vascular characters outlined above, and the palatal  
377 groove/canal system described herein. It is unclear whether encephalic vascular evolution in  
378 Thalattosuchia was stepwise and gradual, or whether one of these characteristics was a ‘key  
379 adaptation’ that triggered rapid change within the thalattosuchian skull. Only new fossil  
380 discoveries, of taxa basal to the teleosauroid-metriorhynchoid split, will allow us to understand  
381 this radical reorganisation.

382         Regardless of what selection pressures drove basal thalattosuchians to evolve these  
383 encephalic vascular characteristics, we posit that within Metriorhynchoidea, as the clade became  
384 increasingly aquatic, these characteristics made the evolution of larger orbits, larger cerebral  
385 hemispheres, and an elevated metabolism ~~possible~~. An elevated metabolism and a pathway to  
386 help maintain stable brain and eye temperatures would also have made feeding below the  
387 thermocline viable, especially in a group considered to be primarily vision-based hunters  
388 (Massare, 1988; Martill *et al.*, 1994; Young *et al.*, 2010; Bowman *et al.*, 2022). Isotopic analyses  
389 suggest that belemnites lived below the thermocline during the Jurassic (e.g. Jenkyns *et al.*,

390 2012; Xu *et al.*, 2018), and an abundance of belemnite hooklets have been found within the body  
391 cavity of Middle Jurassic metriorhynchids from the Oxford Clay Formation of the UK (Martill,  
392 1986). While the evolution of hypertrophied salt glands has been cited as an example of how  
393 physiological changes expanded the metriorhynchid prey envelope, to include osmoconforming  
394 species (Fernández & Gasparini, 2000, 2008; Cowgill *et al.*, 2022a), thermophysiological  
395 changes were undoubtedly also exceptionally important. The suite of vascular characters outlined  
396 herein are unique to thalattosuchians, and no other crocodylomorph clade contained a lineage  
397 that evolved to become fully aquatic. Perhaps these changes in cranial vasculature were a  
398 necessary precursor for the development of the fully aquatic metriorhynchids.

399

## 400 CONCLUSIONS

401 Herein we show that the palatal grooves of thalattosuchians were unique within  
402 Crocodylomorpha. We cannot find any other crocodylomorph clade that had anteroposteriorly  
403 aligned grooves along their maxilla and palatines, and cannot find any evidence that the absence  
404 of the grooves is influenced by ontogeny. Based on CT scans of thalattosuchian skulls, these  
405 grooves are continuous with a pair of canals which travel through the palatines connecting the  
406 oral and nasal cavities. The canals open into the **posterior terminus of the grooves** via foramina  
407 (best seen in Fig. 1B). These internal canals are also not present in the CT scans of extant  
408 crocodylian skulls.

409         However, the palatal canals, foramina and grooves are strikingly similar to those of  
410 another group, cetaceans. Present in both fossil semi-aquatic species, and fossil and extant fully  
411 aquatic species, these structures transmit the greater palatine artery which supplies a palatal  
412 venous thermoregulatory structure. Given the convergence in palatal grooves between these

413 groups, we hypothesise that the canals and grooves of thalattosuchians transmitted hypertrophied  
414 vasculature. Based on the position of the canal/groove system, the most likely candidate are the  
415 medial nasal vessels. Connecting the medial nasal vessels to the palatal vascular plexus would  
416 have created a novel heat exchange pathway, one that linked the plexus (an important  
417 thermoregulatory site) to the vessels that supply blood to the brain and eyes. As thalattosuchians  
418 likely had increased cephalic blood volume and flow rates relative to other crocodylomorphs, a  
419 corresponding increase in cephalic thermoregulatory capabilities would be necessary. However,  
420 at present we cannot ascertain which came first: increased blood flow (e.g. wider cerebral carotid  
421 canal and external foramina), increased blood volume (e.g. orbital canals almost as wide as the  
422 carotid canals, and hypertrophied pituitary fossa chamber, transverse dural venous sinuses and  
423 stapedia canals), or the medial nasal vessel mediated thermoregulatory pathway. We also do not  
424 know the rate and order at which these changes occurred. New fossil discoveries are needed to  
425 elucidate thalattosuchian cephalic vascular evolution.

426

## 427 **ACKNOWLEDGEMENTS**

428 We thank S. Maidment (NHMUK), Z. Timmons (NMS) R. Allain (MNHN), and M. Gasparik  
429 and Z. Szentesi (MTM) for providing generous access to the specimens in their care, M. Johnson  
430 (Stuttgart) for providing photograph of the Chinese teleosaurid and S. Sachs (Bielefeld) for  
431 generously helping with the NMS figures. The funders had no role in study design, data  
432 collection and analysis, decision to publish, or preparation of the manuscript.

433

## 434 **REFERENCES**



- 435 **Adams TL. 2013.** A new neosuchian crocodyliform from the Lower Cretaceous (late Aptian)  
436 Twin Mountains Formation of north-central Texas. *Journal of Vertebrate Paleontology*  
437 **33**:85–101
- 438 **Aiglstorfer M, Havlik P, Herrera Y. 2020.** The first metriorhynchoid crocodyliform from the  
439 Aalenian (Middle Jurassic) of Germany, with implications for the evolution of  
440 Metriorhynchoidea. *Zoological Journal of the Linnean Society* **188**:522–551
- 441 **Andrade MB, Bertini RJ. 2008.** A new *Sphagesaurus* (Mesoeucrocodylia: Notosuchia) from  
442 the Upper Cretaceous of Monte Alto City (Bauru Group, Brazil), and a revision of the  
443 Sphagesauridae. *Historical Biology* **20**(2):101–136
- 444 **Andrews CW. 1913.** *A descriptive catalogue of the marine reptiles of the Oxford Clay, Part*  
445 *Two*. P. xxiv + 206. 13 pl. British Museum (Natural History), London
- 446 **Bajpai S, Thewissen JGM, Conley RW. 2011.** Cranial anatomy of middle Eocene  
447 *Remingtonocetus* (Cetacea, Mammalia) from Kutch, India. *Journal of Paleontology* **85**:703–  
448 718
- 449 **Barbosa JA, Kellner AWA, Viana MSS. 2008.** New dyrosaurid crocodylomorph and evidences  
450 for faunal turnover at the K–P transition in Brazil. *Proceeding of the Royal Society B*  
451 **275**(1641):1385–1391
- 452 **Berta A. 1991.** New *Enaliarctos*\* (Pinnipedimorpha) from the Oligocene and Miocene of  
453 Oregon and the role of ‘enaliarctids’ in pinniped phylogeny. *Smithsonian Contributions to*  
454 *Paleobiology* **69**:1–33
- 455 **Bianucci B, Gingerich PD. 2011.** *Aegyptocetus tarfa*, n. gen. et sp. (Mammalia, Cetacea), from  
456 the middle Eocene of Egypt: clinorhynch, olfaction, and hearing in a protocetid whale.  
457 *Journal of Vertebrate Paleontology* **31**:1173–1188

- 458 **Bowman CIW, Young MT, Schwab JA, Walsh S, Witmer LM, Herrera Y, Choiniere J,**  
459 **Dollman K, Brusatte SL. 2022.** Rostral neurovasculature indicates sensory trade-offs in  
460 Mesozoic pelagic crocodylomorphs. *The Anatomical Record* **305**:2654–2669
- 461 **Brusatte SL, Muir A, Young MT, Walsh S, Steel L, Witmer LM. 2016.** The braincase and  
462 neurosensory anatomy of an Early Jurassic marine crocodylomorph: implications for  
463 crocodylian sinus evolution and sensory transitions. *The Anatomical Record* **299**:1511–1530
- 464 **Carvalho IS, Campos ACA, Nobre PH. 2005.** *Baurusuchus salgadoensis*, a new  
465 Crocodylomorpha from the Bauru Basin (Cretaceous), Brazil. *Gondwana Research* **8**(1):11–  
466 30
- 467 **Carvalho IS, Teixeira VPA, Ferraz MLF, Ribeiro LCB, Martinelli AG, Neto FM, Sertich**  
468 **JJW, Cunha GC, Cunha IC, Ferraz PF. 2011.** *Campinasuchus dinizi* gen. et sp. nov., a  
469 new Late Cretaceous baurusuchid (Crocodyliformes) from the Bauru Basin, Brazil. *Zootaxa*  
470 **2871**:19–42
- 471 **Carvalho IS, Vasconcellos FM, Tavares SAS. 2007.** *Montealtosuchus arrudacamposi*, a new  
472 peirosaurid crocodile (Mesoeucrocodylia) from the Late Cretaceous Adamantina Formation  
473 of Brazil. *Zootaxa* **1607**:35–46
- 474 **Churchill M, Martinez-Caceres M, de Muizon C, Mnieckowski J, Geisler JH. 2016.** The  
475 Origin of high frequency hearing in whales. *Current Biology* **26**:2144–2149
- 476 **Cowgill T, Young MT, Schwab JA, Walsh S, Witmer LM, Herrera Y, Dollman KN, Turner**  
477 **AH, Brusatte SL. 2022a.** Cephalic salt gland evolution in Mesozoic pelagic  
478 crocodylomorphs. *Zoological Journal of the Linnean Society* zlac027

- 479 **Cowgill T, Young MT, Schwab JA, Walsh S, Witmer LM, Herrera Y, Dollman K,**  
480 **Choiniere J, Brusatte SL. 2022b.** Paranasal sinus system and upper respiratory tract  
481 evolution in Mesozoic pelagic crocodylomorphs. *The Anatomical Record* **305**:2583–2603
- 482 **Delfino M, Codrea V, Folie A, Dica P, Godefroit P, Smith T. 2008.** A complete skull of  
483 *Allodaposuchus precedens* Nopcsa, 1928 (Eusuchia) and a reassessment of the morphology  
484 of the taxon based on the Romanian remains. *Journal of Vertebrate Paleontology* **28**(1):111–  
485 122
- 486 **Delfino M, Piras P, Smith T. 2005.** Anatomy and phylogeny of the gavialoid crocodylian  
487 *Eosuchus lerichei* from the Paleocene of Europe. *Acta Palaeontologica Polonica* **50**(3):565–  
488 580
- 489 **Deméré TA, McGowen MR, Berta A, Gatesy J. 2008.** Morphological and molecular evidence  
490 for a stepwise evolutionary transition from teeth to baleen in mysticete whales. *Systematic*  
491 *Biology* **57**:15–37
- 492 **Dewaele L, Lambert O, Louwye S. 2018.** A critical revision of the fossil record, stratigraphy  
493 and diversity of the Neogene seal genus *Monotherium* (Carnivora, Phocidae). *Royal Society*  
494 *Open Science* **5**:171669
- 495 **Dollman KN, Clark JM, Norell MA, Xing X, Choiniere JN. 2018.** Convergent evolution of a  
496 eusuchian-type secondary palate within Shartegosuchidae. *American Museum Novitates*  
497 **3901**:1–23
- 498 **Ekdale EG, Deméré TA. 2022.** Neurovascular evidence for a co-occurrence of teeth and baleen  
499 in an Oligocene mysticete and the transition to filter-feeding in baleen whales. *Zoological*  
500 *Journal of the Linnean Society* **194**:395–415

- 501 **Ekdale EG, Deméré TA, Berta A. 2015.** Vascularization of the grey whale palate (Cetacea,  
502 Mysticeti, *Eschrichtius robustus*): soft tissue evidence for an alveolar source of blood to  
503 baleen. *Journal of Anatomical Research* **298**:691–702
- 504 **Erb A, Turner AH. 2021.** Braincase anatomy of the Paleocene crocodyliform *Rhabdognathus*  
505 revealed through high resolution computed tomography. *PeerJ* **9**:e11253
- 506 **Fernández, M. and Gasparini, Z. 2000.** Salt glands in a Tithonian metriorhynchid  
507 crocodyliform and their physiological significance. *Lethaia* **33**:269–276
- 508 **Fernández M, Gasparini Z. 2008.** Salt glands in the Jurassic metriorhynchid *Geosaurus*:  
509 implications for the evolution of osmoregulation in Mesozoic marine crocodyliforms.  
510 *Naturwissenschaften* **95**:79–84
- 511 **Fernández MS, Herrera Y. 2009.** Paranasal sinus system of *Geosaurus araucanensis* and the  
512 homology of the antorbital fenestra of metriorhynchids (Thalattosuchia: Crocodylomorpha).  
513 *Journal of Vertebrate Paleontology* **29**:702–714
- 514 **Fernández MS, Carabajal AP, Gasparini Z, Chong Diaz G. 2011.** A metriorhynchid  
515 crocodyliform braincase from northern Chile. *Journal of Vertebrate Paleontology* **31**:369–  
516 377
- 517 **Foffa D, Young MT. 2014.** The cranial osteology of *Tyrannoneustes lythrodectikos*  
518 (Crocodylomorpha: Metriorhynchidae) from the Middle Jurassic of Europe. *PeerJ* **2**:e608
- 519 **Ford Jr TJ, Kraus SD. 1992.** A rete in the right whale. *Nature* **359**:680
- 520 **Ford Jr TJ, Werth AJ, George JC. 2013.** An intraoral thermoregulatory organ in the bowhead  
521 whale (*Balaena mysticetus*), the corpus cavernosum maxillaris. *The Anatomical Record*  
522 **296**:701–708

- 523 **Fordyce RE. 2002.** *Simocetus rayi* (Odontoceti, Simocetidae, new family); a bizarre new archaic  
524 Oligocene dolphin from the eastern North Pacific. *Smithsonian Contributions to*  
525 *Paleobiology* **93**:185–222
- 526 **Fortier D, Perea D, Schultz C. 2011.** Redescription and phylogenetic relationships of  
527 *Meridiosaurus vallisparadisi*, a pholidosaurid from the Late Jurassic of Uruguay. *Zoological*  
528 *Journal of the Linnean Society* **163**:S257–S272
- 529 **Fraas E. 1902.** Die Meer-Krocodilier (Thalattosuchia) des oberen Jura unter specieller  
530 Berücksichtigung von *Dacosaurus* und *Geosaurus*. *Palaeontographica* **49**:1–72
- 531 **Hastings AK, Bloch JI, Cadena EA, Jaramillo CA. 2010.** A new small short-snouted  
532 dyrosaurid (Crocodylomorpha, Mesoeucrocodylia) from the Paleocene of northeastern  
533 Colombia. *Journal of Vertebrate Paleontology* **30**:139–162
- 534 **Hastings AK, Block JI, Jaramillo CA. 2015.** A new blunt-snouted dyrosaurid, *Anthracosuchus*  
535 *balrogus* gen. et sp. nov. (Crocodylomorpha, Mesoeucrocodylia) from the Palaeocene of  
536 Colombia. *Historical Biology* **27**:998–1020
- 537 **Herrera Y, Vennari VV. 2015.** Cranial anatomy and neuroanatomical features of a new  
538 specimen of Geosaurini (Crocodylomorpha: Metriorhynchidae) from west-central Argentina.  
539 *Historical Biology* **27**:33–41
- 540 **Herrera Y, Fernández MS, Gasparini Z. 2013.** The snout of *Cricosaurus araucanensis*: a case  
541 study in novel anatomy of the nasal region of metriorhynchids. *Lethaia* **46**:331–340
- 542 **Herrera Y, Fernández MS, Lamas SG, Campos L, Talevi M, Gasparini Z. 2017.**  
543 Morphology of the sacral region and reproductive strategies of Metriorhynchidae: a counter-  
544 intuitive approach. *Earth and Environmental Science Transactions of the Royal Society of*  
545 *Edinburgh* **106**:247–255

- 546 **Herrera Y, Leardi JM, Fernández MS. 2018.** Braincase and endocranial anatomy of two  
547 thalattosuchian crocodylomorphs and their relevance in understanding their adaptations to the  
548 marine environment. *PeerJ* **6**:e5686
- 549 **Hua S. 2020.** A new specimen of *Teleidosaurus calvadosii* (Eudes-Deslongchamps, 1866)  
550 (Crocodylia, Thalattosuchia) from the Middle Jurassic of France. *Annales de Paléontologie*  
551 **106**:102423
- 552 **Hua S, Buffetaut E, Legall C, Rogron P. 2007.** *Oceanosuchus boecensis* n. gen, n. sp., a  
553 marine pholidosaurid (Crocodylia, Mesosuchia) from the Lower Cenomanian of Normandy  
554 (western France). *Bulletin de la Société Géologique de France* **178**:503–513
- 555 **Hua S, de Buffrénil V. 1996.** Bone histology as a clue in the interpretation of functional  
556 adaptations in the Thalattosuchia (Reptilia, Crocodylia). *Journal of Vertebrate Paleontology*  
557 **16**:703–717
- 558 **Ichishima H, Sawamura H, Ito H, Otani S, Ishikawa H. 2008.** Do the so-called nutrient  
559 foramina on the palate tell us the presence of baleen plates in toothed mysticetes? In:  
560 Abstracts of the Fifth Conference on Secondary Adaptation of Tetrapods to Life in Water. P  
561 24–25
- 562 **Iijima M, Qiao Y, Lin W, Peng Y, Yoneda M, Liu J. 2022.** An intermediate crocodylian  
563 linking two extant gharials from the Bronze Age of China and its human-induced extinction.  
564 *Proceedings of the Royal Society B* **289**:20220085
- 565 **Jenkyns HC, Schouten-Huibers L, Schouten S, Sinninghe Damsté JS. 2012.** Warm Middle  
566 Jurassic–Early Cretaceous high-latitude sea-surface temperatures from the Southern Ocean.  
567 *Climate of the Past* **8**:215–226

- 568 **Johnson MM, Young MT, Brusatte SL, Thuy B, Weis R. 2019.** A catalogue of teleosauroids  
569 (Crocodylomorpha: Thalattosuchia) from the Toarcian and Bajocian (Jurassic) of southern  
570 Luxembourg. *Historical Biology* **31**(9):1179–1194
- 571 **Johnson MM, Young MT, Brusatte SL. 2020.** The phylogenetics of Teleosauroidea  
572 (Crocodylomorpha, Thalattosuchia) and implications for their ecology and evolution. *PeerJ*  
573 **8**:e9808
- 574 **Jouve S. 2009.** The skull of *Teleosaurus cadomensis* (Crocodylomorpha; Thalattosuchia), and  
575 phylogenetic analysis of Thalattosuchia. *Journal of Vertebrate Paleontology* **29**:88–102
- 576 **Jouve S, Iarochène M, Bouya B, Amaghaz M. 2006.** A new species of *Dyrosaurus*  
577 (Crocodylomorpha, Dyrosauridae) from the early Eocene of Morocco: phylogenetic  
578 implications. *Zoological Journal of the Linnean Society* **148**:603–656
- 579 **Kilgore DL, Boggs DF, Birchard, G.F. 1979.** Role of the rete mirabile ophthalmicum in  
580 maintaining the body-to-brain temperature difference in pigeons. *Journal of Comparative*  
581 *Physiology* **129**:119–122
- 582 **Kley NJ, Sertich JJ, Turner AH, Krause DW, O'Connor PM, Georgi JA. 2010.** Craniofacial  
583 morphology of *Simosuchus clarki* (Crocodyliformes: Notosuchia) from the late Cretaceous of  
584 Madagascar. *Journal of Vertebrate Paleontology* **30**:13–98
- 585 **Koretsky IA, Rahmat SJ. 2021.** Unique short-faced Miocene seal discovered in Grytsiv  
586 (Ukraine). *Zoodyversity* **55**:143–154
- 587 **Larsson HCE, Sues H-D. 2007.** Cranial osteology and phylogenetic relationships of  
588 *Hamadasuchus rebouli* (Crocodyliformes: Mesoeucrocodylia) from the Cretaceous of  
589 Morocco. *Zoological Journal of the Linnean Society* **149**:533–567

- 590 **Martill DM. 1986.** The diet of *Metriorhynchus*, a Mesozoic marine crocodile. *Neues Jahrbuch*  
591 *für Geologie und Palaontologie, Abhandlungen* **173**:621–625
- 592 **Martill DM, Taylor MA, Duff KL, Riding JB, Bown PR. 1994.** The trophic structure of the  
593 biota of the Peterborough Member, Oxford Clay Formation (Jurassic), UK. *Journal of the*  
594 *Geological Society* **151**:173–194
- 595 **Massare JA. 1988.** Swimming capabilities of Mesozoic marine reptiles: Implications for method  
596 of predation. *Paleobiology* **14**:187–205
- 597 **Martin JE, Smith T, Salaviale C, Adrien J, Delfino M. 2020.** Virtual reconstruction of the  
598 skull of *Bernissartia fagesii* and current understanding of the neosuchian–eusuchian  
599 transition. *Journal of Systematic Palaeontology* **18**:1079–1101
- 600 **Meunier LV, Larsson HC. 2017.** Revision and phylogenetic affinities of *Elosuchus*  
601 (Crocodyliformes). *Zoological Journal of the Linnean Society* **179**(1):169–200
- 602 **Midtgård U. 1983.** Scaling of the brain and the eye cooling system in birds: a morphometric  
603 analysis of the rete ophthalmicum. *Journal of Experimental Zoology* **225**:197–207
- 604 **Midtgård U. 1984.** Blood vessels and the occurrence of arteriovenous anastomoses in cephalic  
605 heat loss areas of mallards, *Anas platyrhynchos* (Aves). *Zoomorphology* **104**:323–335
- 606 **de Muizon C, Domning DP, Ketten DR. 2002.** *Odobenocetops peruvianus*, the Walrus-  
607 convergent delphinoid (Mammalia: Cetacea) from the Early Pliocene of Peru. *Smithsonian*  
608 *Contributions to Paleobiology* **93**:223–262
- 609 **Narváez I, Brochu CA, Escaso F, Pérez-García A, Ortega F. 2015.** New crocodyliforms from  
610 Southwestern Europe and definition of a diverse clade of European Late Cretaceous basal  
611 eusuchians. *PLoS ONE* **10**(11):e0140679



- 612 **Novas FE, Pais DF, Pol D, Carvalho IS, Scanferla A, Mones A, Suárez Riglos M. 2009.**  
613 Bizarre notosuchian crocodyliform with associated eggs from the Upper Cretaceous of  
614 Bolivia. *Journal of Vertebrate Paleontology* **29**:1316–1320
- 615 **Ósi A, Clark JM, Weishampel DB. 2007.** First report on a new basal eusuchian crocodyliform  
616 with multicusped teeth from the Upper Cretaceous (Santonian) of Hungary. *Neues Jahrbuch*  
617 *für Geologie und Paläontologie, Abhandlungen* **243**:169–177
- 618 **Ósi A, Young MT, Galácz A, Rabi M. 2018.** A new large-bodied thalattosuchian crocodyliform  
619 from the Lower Jurassic (Toarcian) of Hungary, with further evidence of the mosaic  
620 acquisition of marine adaptations in Metriorhynchoidea. *PeerJ* **6**:e4668
- 621 **Parrilla-Bel J, Young MT, Moreno-Azanza M, Canudo JI. 2013.** The first metriorhynchid  
622 crocodyliform from the Middle Jurassic of Spain, with implications for evolution of the  
623 subclade Rhacheosaurini. *PLOS ONE* **8**(1):e54275
- 624 **Pierce SE, Benton MJ, 2006.** *Pelagosaurus typus* Bronn, 1841 (Mesoeucrocodylia:  
625 Thalattosuchia) from the Upper Lias (Toarcian, Lower Jurassic) of Somerset, England.  
626 *Journal of Vertebrate Paleontology* **26**:621–635
- 627 **Pierce SE, Williams M, Benson RBJ. 2017.** Virtual reconstruction of the endocranial anatomy  
628 of the early Jurassic marine crocodylomorph *Pelagosaurus typus* (Thalattosuchia). *PeerJ*  
629 **5**:e3225
- 630 **Pol D. 2003.** New remains of *Sphagesaurus* (Crocodylomorpha: Mesoeucrocodylia) from the  
631 Upper Cretaceous of Brazil. *Journal of Vertebrate Paleontology* **23**(4):817–831
- 632 **Pol D, Gasparini Z. 2009.** Skull anatomy of *Dakosaurus andiniensis* (Thalattosuchia:  
633 Crocodylomorpha) and the phylogenetic position of Thalattosuchia. *Journal of Systematic*  
634 *Palaeontology* **7**:163–197

- 635 **Porter WR, Witmer LM. 2015.** Vascular patterns in iguanas and other squamates: blood  
636 vessels and sites of thermal exchange. *PLoS ONE* **10**:e0139215
- 637 **Porter WR, Witmer LM. 2016.** Avian cephalic vascular anatomy, sites of thermal exchange,  
638 and the rete ophthalmicum. *The Anatomical Record* **299**:1461–1486
- 639 **Porter WR, Sedlmayr JC, Witmer LM. 2016.** Vascular patterns in the heads of crocodylians:  
640 blood vessels and sites of thermal exchange. *Journal of Anatomy* **229**:800–824
- 641 **Pritchard AC, Turner AH, Allen ER, Norell MA. 2013.** Osteology of a North American  
642 goniopholidid (*Eutretauranosuchus delfsi*) and palate evolution in Neosuchia. *American*  
643 *Museum Novitates* **3783**:1–56
- 644 **Rio JP, Mannion PD, Tschopp E, Martin JE, Delfino M. 2020.** Reappraisal of the  
645 morphology and phylogenetic relationships of the alligatoroid crocodylian *Diplocynodon*  
646 *hantoniensis* from the late Eocene of the United Kingdom. *Zoological Journal of the Linnean*  
647 *Society* **188**:579–629
- 648 **Ristevski J, Young MT, Andrade MB, Hastings AK. 2018.** A new species of  
649 *Anteophthalmosuchus* (Crocodylomorpha, Goniopholididae) from the Lower Cretaceous of  
650 the Isle of Wight, United Kingdom, and a review of the genus. *Cretaceous Research* **84**:340–  
651 383
- 652 **Rule JR, Adams JW, Rovinsky DS, Hocking DP, Evans AR, Fitzgerald EMG. 2020.** A new  
653 large-bodied Pliocene seal with unusual cutting teeth. *Royal Society Open Science* **7**:201591
- 654 **Salisbury SW, Molnar RE, Frey E, Willis P. 2006.** The origin of modern crocodyliforms: new  
655 evidence from the Cretaceous of Australia. *Proceedings of the Royal Society B* **273**:2439–  
656 2448

- 657 **Salisbury SW, Naish D. 2011.** Crocodylians. In: Batten, D., Lane, P.D. (eds). *English Wealden*  
658 *fossils*. Palaeontological Association, Aberystwyth, 305–369
- 659 **Seymour RS, Hu Q, Snelling EP, White CR. 2019.** Interspecific scaling of blood flow rates  
660 and arterial sizes in mammals. *Journal of Experimental Biology* **222**(7): jeb199554
- 661 **Schwab JA, Young MT, Neenan JM, Walsh SA, Witmer LM, Herrera Y, Allain R, Brochu**  
662 **CA, Choiniere JN, Clark JM, Dollman KN, Etches S, Fritsch G, Gignac PM,**  
663 **Ruebenstahl A, Sachs S, Turner AH, Vignaud P, Wilberg EW, Xu X, Zanno LE,**  
664 **Brusatte SL. 2020.** Inner ear sensory system changes as extinct crocodylomorphs  
665 transitioned from land to water. *Proceedings of the National Academy of Sciences*  
666 **117**:10422–10428
- 667 **Schwab JA, Young MT, Herrera Y, Witmer LM, Walsh S, Katsamenis OL, Brusatte SL.**  
668 **2021.** The braincase and inner ear of ‘*Metriorhynchus*’ cf. *brachyrhynchus* – implications for  
669 aquatic sensory adaptations in crocodylomorphs. *Journal of Vertebrate Paleontology*  
670 **41**:e1912062
- 671 **Séon N, Amiot R, Martin JE, Young MT, Middleton H, Fourel F, Picot L, Valentin X,**  
672 **Lécuyer C. 2020.** Thermophysiologicals of Jurassic marine crocodylomorphs inferred from the  
673 oxygen isotope composition of their tooth apatite. *Philosophical Transactions of the Royal*  
674 *Society B* **375**:2019–2039
- 675 **Sereno PC, Larsson HCE. 2009.** Cretaceous Crocodyliforms from the Sahara. *ZooKeys* **28**:1–  
676 143
- 677 **Spindler F, Lauer R, Tischlinger H, Mäuser M. 2021.** The integument of pelagic  
678 crocodylomorphs (Thalattosuchia: Metriorhynchidae). *Palaeontologia Electronica* **24**:a25

- 679 **Sweetman SC, Pedreira-Segade U, Vidovic SU. 2015.** A new bernissartiid crocodyliform from  
680 the Lower Cretaceous Wessex Formation (Wealden Group, Barremian) of the Isle of Wight,  
681 southern England. *Acta Palaeontologica Polonica* **60**:257–268
- 682 **Turner AH. 2015.** A review of *Shamosuchus* and *Paralligator* (Crocodyliformes, Neosuchia)  
683 from the Cretaceous of Asia. *PLOS ONE* **10**:e0118116
- 684 **Tykoski RS, Rowe TB, Ketcham RA, Colbert MW. 2002.** *Calsoyasuchus valliceps*, a new  
685 crocodyliform from the Early Jurassic Kayenta Formation of Arizona. *Journal of Vertebrate*  
686 *Paleontology* **22**:593–611
- 687 **Vélez-Juarbe J, Pyenson ND. 2012.** *Bohaskaia monodontoides*, a new monodontid (Cetacea,  
688 Odontoceti, Delphinoidea) from the Pliocene of the western North Atlantic Ocean. *Journal of*  
689 *Vertebrate Paleontology* **32**:476–484
- 690 **Werth AJ. 2007.** Adaptations of the cetacean hyolingual apparatus for aquatic feeding and  
691 thermoregulation. *The Anatomical Record* **290**:546–568
- 692 **Wharton DS. 2000.** An enlarged endocranial venous system in *Steneosaurus pictaviensis*  
693 (Crocodylia: Thalattosuchia) from the Upper Jurassic of Les Lourdines, France. *Comptes*  
694 *Rendus de l'Académie des Sciences – Series IIA – Earth and Planetary Science* **331**(3):221–  
695 226
- 696 **Wilberg EW. 2015.** A new metriorhynchoid (Crocodylomorpha, Thalattosuchia) from the  
697 Middle Jurassic of Oregon and the evolutionary timing of marine adaptations in  
698 thalattosuchian crocodylomorphs. *Journal of Vertebrate Paleontology* **35**:e902846
- 699 **Wilberg EW, Beyl AR, Pierce SE, Turner AH. 2022.** Cranial and endocranial anatomy of a  
700 three-dimensionally preserved teleosauroid thalattosuchian skull. *The Anatomical Record*  
701 **305**:2620–2653

- 702 **Xu W, Ruhl M, Jenkyns HC, Leng MJ, Huggett JM, Minisini D, Ullmann CV, Riding JB,**  
703 **Weijers JWH, Storm MS, Percival LME, Tosca NJ, Idiz EF, Tegelaar EW, Hesselbo**  
704 **SP. 2018.** Evolution of the Toarcian (Early Jurassic) carbon-cycle and global climatic  
705 controls on local sedimentary processes (Cardigan Bay Basin, UK). *Early and Planetary*  
706 *Science Letters* **484**:396–411
- 707 **Wu X-C, Cheng ZW, Russell AP, Cumbaa SL. 2001.** Cranial anatomy of a new crocodyliform  
708 (Archosauria: Crocodylomorpha) from the Lower Cretaceous of Song-Liao Plain,  
709 northeastern China. *Canadian Journal of Earth Sciences* **38**:1653–1663
- 710 **Young MT, Andrade MB, Etches S, Beatty BL. 2013.** A new metriorhynchid crocodylomorph  
711 from the Lower Kimmeridge Clay Formation (Late Jurassic) of England, with implications  
712 for the evolution of dermatocranium ornamentation in Geosaurini. *Zoological Journal of the*  
713 *Linnean Society* **169**:820–848
- 714 **Young MT, Brignon A, Sachs S, Hornung J, Foffa D, Kitson JJN, Johnson MM, Steel L.**  
715 **2021.** Cutting the Gordian knot: a historical and taxonomic revision of the Jurassic  
716 crocodylomorph *Metriorhynchus*. *Zoological Journal of the Linnean Society* **192**(2):510–553
- 717 **Young MT, Brusatte SL, Andrade MB, Desojo JB, Beatty BL, Steel L, Fernández MS,**  
718 **Sakamoto M, Ruiz-Omeñaca JI, Schoch RR. 2012.** The cranial osteology and feeding  
719 ecology of the metriorhynchid crocodylomorph genera *Dakosaurus* and *Plesiosuchus* from  
720 the Late Jurassic of Europe. *PLOS ONE* **7**:e44985
- 721 **Young MT, Brusatte SL, Ruta M, Andrade MB. 2010.** The evolution of Metriorhynchoidea  
722 (Mesoeucrocodylia, Thalattosuchia): an integrated approach using geometrics  
723 morphometrics, analysis of disparity and biomechanics. *Zoological Journal of the Linnean*  
724 *Society* **158**:801–859

- 725 **Young MT, Foffa D, Steel L, Etches S. 2020b.** Macroevolutionary trends in the genus  
726 *Torvoneustes* (Croodylomorpha: Metriorhynchidae) and discovery of a giant specimen from  
727 the Late Jurassic of Kimmeridge, UK. *Zoological Journal of the Linnean Society* **189**(2):483–  
728 493
- 729 **Young MT, Sachs S, Abel P, Foffa D, Herrera Y, Kitson JJN. 2020a.** Convergent evolution  
730 and possible constraint in the posterodorsal retraction of the external nares in pelagic  
731 croodylomorphs. *Zoological Journal of the Linnean Society* **189**(2):494–520  
732

733

## Figures

734

735 **FIGURE 1.** Comparison of the palatal grooves in different thalattosuchian clades, skulls shown  
736 in palatal view. (A) IVPP V 10098, Chinese teleosaurid; (B) NHMUK PV OR 32599, the early-  
737 diverging metriorhynchoid *Pelagosaurus typus*; (C) NHMUK PV R 3700, the metriorhynchid  
738 ‘*Metriorhynchus*’ *brachyrhynchus*. Abbreviations: PG, palatal groove; SOG, suborbital groove.

739 **Planned for full page width.**

740

741 **FIGURE 2.** Comparison between the thalattosuchian and extant crocodylians studied, CT  
742 reconstructions of the skulls shown in palatal view. (A) NHMUK PV OR 32599, the early-  
743 diverging metriorhynchoid *Pelagosaurus typus*; (B) MLP 72-IV-7-1, the metriorhynchid  
744 *Cricosaurus araucanensis*; (C) UF herp 118998, the gavialid *Gavialis gangeticus*; (D) TMM  
745 M983, the alligatorid *Alligator mississippiensis*. Abbreviations: PG, palatal groove.

746 **Planned for full page width.**

747

748 **FIGURE 3.** Comparison of the extant crocodylians studied, CT reconstructions of the skulls  
749 shown in palatal view. Note, none of the extant crocodylians have palatal grooves. (A) OUVC  
750 10606, hatchling specimen of *Alligator mississippiensis*; (B) OUVC 9761, juvenile specimen of  
751 *Alligator mississippiensis*; (C) OUVC 11415, juvenile specimen of *Alligator mississippiensis*;  
752 (D) TMM M-983, juvenile specimen of *Alligator mississippiensis*; (E) USNM 211233, adult  
753 specimen of *Alligator mississippiensis*; (F) FMNH 73711, subadult specimen of *Caiman*  
754 *crocodilus*; (G) FMNH 59071, adult specimen of *Crocodylus acutus*; (H) MNB AB50.071, adult  
755 specimen of *Crocodylus rhombifer*; (I) TMM M-4980, adult specimen of *Crocodylus moreletii*;  
756 (J) OUVC 10899, juvenile specimen of *Crocodylus porosus*; (K) FMNH 98936, adult specimen

757 of *Osteolaemus tetraspis*; (L) TMM M-6807, subadult specimen of *Crocodylus johnstoni*; (M)  
758 TMM M-3529, adult specimen of *Mecistops cataphractus*; (N) TMM M-5490, subadult  
759 specimen of *Gavialis gangeticus*; (O) UF herp 118998, adult specimen of *Gavialis gangeticus*;  
760 (P) TMM M-6342, subadult specimen of *Tomistoma schlegelii*; (Q) USNM 211322, adult  
761 specimen of *Tomistoma schlegelii*.

762 **Planned for full page width.**

763

764 **FIGURE 4.** The early-diverging teleosauroid *Plagiophthalmosuchus gracilirostris* (NHMUK  
765 PV OR 15500), from the early Toarcian of the UK. (A) snout coronal view showing the position  
766 of the palatal canals. Three-dimensional reconstruction of the skull in (B) dorsal, and (C) lateral  
767 view, both showing the palatal canals in red and the CT slice of (A) shown in blue.

768 Abbreviations: Alv, alveolus; DAC, dorsal alveolar canal; PC, palatal canal.

769 **Planned for full page width.**

770

771 **FIGURE 5.** The early-diverging metriorhynchoid *Pelagosaurus typus* (NHMUK PV OR 32599)  
772 referred specimen, early Toarcian of France. (A) snout coronal view showing the position of the  
773 palatal canals. Three-dimensional reconstruction of the skull in (B) dorsal, and (C) lateral view,  
774 both showing the palatal canals in red and the CT slice of (A) shown in blue. Abbreviations: Alv,  
775 alveolus; DAC, dorsal alveolar canal; PC, palatal canal.

776 **Planned for full page width.**

777

778 **FIGURE 6.** The early-diverging metriorhynchoid *Eoneustes gaudryi* (NHMUK PV R 3263)  
779 holotype, Bathonian of France. (A) snout coronal view showing the position of the palatal canals.  
780 Three-dimensional reconstruction of the skull in (B) dorsal, and (C) lateral view, both showing



781 the palatal canals in red and the CT slice of (A) shown in blue. Abbreviations: Alv, alveolus;  
782 DAC, dorsal alveolar canal; PC, palatal canal.

783 **Planned for full page width.**

784

785 **FIGURE 7.** The metriorhynchid *Thalattosuchus superciliosus* (NHMUK PV R 11999) referred  
786 specimen, middle Callovian of the UK. (A) snout coronal view showing the position of the  
787 palatal canals. Three-dimensional reconstruction of the skull in (B) dorsal, and (C) lateral view,  
788 both showing the palatal canals in red and the CT slice of (A) shown in blue. Abbreviations: Alv,  
789 alveolus; DAC, dorsal alveolar canal; PC, palatal canal.

790 **Planned for full page width.**

791

792 **FIGURE 8.** The metriorhynchid *Cricosaurus araucanensis* (MLP 72-IV-7-1) holotype,  
793 Tithonian of Argentina. (A) snout coronal view showing the position of the palatal canals. Three-  
794 dimensional reconstruction of the skull in (B) dorsal, and (C) lateral view, both showing the  
795 palatal canals in red and the CT slice of (A) shown in blue. Abbreviations: Alv, alveolus; DAC,  
796 dorsal alveolar canal; PC, palatal canal.

797 **Planned for full page width.**

798

799 **FIGURE 9.** The metriorhynchid *Cricosaurus schroederi* (MM Pa1), from the early Valanginian  
800 of Germany. (A) snout coronal view showing the position of the palatal canals. Three-  
801 dimensional reconstruction of the skull in (B) dorsal, and (C) lateral view, both showing the  
802 palatal canals in red and the CT slice of (A) shown in blue. Abbreviations: Alv, alveolus; DAC,  
803 dorsal alveolar canal; PC, palatal canal.

804 **Planned for full page width.**

805

806 **FIGURE 10.** The extant gavialid *Gavialis gangeticus* (UF-herp-118998). (A) snout coronal view  
807 showing the lack of palatal canals. Three-dimensional reconstruction of the skull in (B) dorsal,  
808 and (C) lateral view, both showing the palatal canals in red and the CT slice of (A) shown in  
809 blue. Abbreviations: Ant, antorbital pneumatic sinus; Alv, alveolus; DAC, dorsal alveolar canal;  
810 Nas, nasal cavity.

811 **Planned for full page width.**

812

813 **FIGURE 11.** The extant alligatorid *Alligator mississippiensis* (USNM 211233). (A) snout  
814 coronal view showing the lack of palatal canals. Three-dimensional reconstruction of the skull in  
815 (B) dorsal, and (C) lateral view, both showing the palatal canals in red and the CT slice of (A)  
816 shown in blue. Abbreviations: Ant, antorbital pneumatic sinus; Alv, alveolus; Nas, nasal cavity.

817 **Planned for full page width.**

818

819 **FIGURE 12.** The extant humpback whale (*Megaptera novaeangliae*). (A) skull showing the  
820 palate, due to size the skull it is shown at an angle; (B) a close-up on the right palatal groove.  
821 Abbreviations: PG, palatal groove.

822 **Planned for full page width.**

823

824 **FIGURE 13.** Comparison of the palatal grooves in different extant odontocete cetaceans, skulls  
825 shown in palatal view. (A) Cuvier's beaked whale (*Ziphius cavirostris*) NMS 2020.9.26; (B)  
826 killer whale (*Orcinus orca*) NMS Z.2015.179. Abbreviations: PG, palatal groove.

827 **Planned for full page width.**

828

829 **FIGURE 14.** Comparison of the palatal grooves in different extant pinnipeds, skulls shown in  
830 palatal view. (A) the Antarctic fur seal (*Arctocephalus gazella*) NMS 2007.91.10; (B) the  
831 Leopard seal (*Hydrurga leptonyx*) NMS 1822.240.T29; (C) the Harbour seal (*Phoca vitulina*)  
832 NMS 1996.99.13. (A) is an otariid, while (B) and (C) are phocids. Abbreviations: PG, palatal  
833 groove.

834 **Planned for full page width.**

835

836 **FIGURE 15.** The extant alligatorid *Alligator mississippiensis* (OUVC 9757) in dorsal view.  
837 Cephalic vasculature with the medial nasal artery/vein shown in yellow and the palatine  
838 artery/vein and palatal plexus shown in red, (A) with the transparent skull, and (B) just the  
839 vasculature. Abbreviations: a+vMedNas, medial nasal artery and vein; a+vPal, palatine artery  
840 and vein; a+vPPlex, arterial and venous palatal plexus.

841 **Planned for full page width.**

842

843 **FIGURE 16.** The extant alligatorid *Alligator mississippiensis* (OUVC 9757) in lateral view.  
844 Cephalic vasculature with the medial nasal artery/vein shown in yellow and the palatine  
845 artery/vein and palatal plexus shown in red, (A) with the transparent skull, and (B) just the  
846 vasculature. Abbreviations: a+vMedNas, medial nasal artery and vein; a+vPal, palatine artery  
847 and vein; a+vPPlex, arterial and venous palatal plexus.

848 **Planned for full page width.**

**Table 1** (on next page)

List of specimens examined herein.

1 **TABLE 1.** List of specimens examined herein.

<b>Species</b>	<b>Specimen number</b>	<b>Age</b>	<b>Voxel size (mm)</b>	<b>Facility/Source</b>
<i>Alligator mississippiensis</i>	OUVC 10606	Recent	0.045	Ohio University MicroCT Facility, USA
<i>Alligator mississippiensis</i>	OUVC 9761	Recent	0.5 X 1	Ohio Health O'Bleness Hospital, USA
<i>Alligator mississippiensis</i>	OUVC 11415	Recent	0.0493	Ohio University MicroCT Facility, USA
<i>Alligator mississippiensis</i>	TMM M983	Recent	0.25 X 0.48	High-Resolution X-ray CT facility, University of Texas, USA
<i>Alligator mississippiensis</i>	USNM 211233	Recent	0.625	Ohio Health O'Bleness Hospital, USA
<i>Caiman crocodilus</i>	FMNH 73711	Recent	0.065 X 0.142	High-Resolution X-ray CT facility, University of Texas, USA
<i>Crocodylus acutus</i>	FMNH 59071	Recent	0.625	Ohio Health O'Bleness Hospital, USA
<i>Crocodylus rhombifer</i>	MNB AB50.0171	Recent	0.1748 X 0.5	High-Resolution X-ray CT facility, University of Texas, USA
<i>Crocodylus moreletii</i>	TMM M-4980	Recent	0.1904 X 0.5	High-Resolution X-ray CT facility, University of Texas, USA
<i>Crocodylus porosus</i>	OUVC 10899	Recent	0.0472	Ohio Health O'Bleness Hospital, USA
<i>Osteolaemus tetraspis</i>	FMNH 98936	Recent	0.0546875 X 0.1108	High-Resolution X-ray CT facility, University of Texas, USA
<i>Crocodylus johnstoni</i>	TMM M-6807	Recent	0.223	High-Resolution X-ray CT facility, University of Texas, USA

<i>Mecistops cataphractus</i>	TMM M-3529	Recent	0.165 X 0.5	High-Resolution X-ray CT facility, University of Texas, USA
<i>Gavialis gangeticus</i>	TMM M-5490	Recent	0.228	High-Resolution X-ray CT facility, University of Texas, USA
<i>Gavialis gangeticus</i>	UF-herp-118998	Recent	0.14654672	Florida Museum of Natural History, USA
<i>Tomistoma schlegelii</i>	USNM 211322	Recent	0.625	Ohio Health O'Bleness Hospital, USA
<i>Tomistoma schlegelii</i>	TMM M-6342	Recent	0.165 X 0.46	High-Resolution X-ray CT facility, University of Texas, USA
<i>Plagiophthalmosuchus gracilirostris</i>	NHMUK PV OR 15500	Toarcian	0.236872 X 0.1185	μVIS X-Ray Imaging Centre, University of Southampton, UK
<i>Pelagosaurus typus</i>	NHMUK PV OR 32599	Toarcian	0.098627983	Nikon XT H 225S CT system, Natural History Museum, London, UK
<i>Eoneustes gaudryi</i>	NHMUK PV R 3263	Bathonian	0.159849	μVIS X-Ray Imaging Centre, University of Southampton, UK
<i>Thalattosuchus superciliosus</i>	NHMUK PV R 11999	Callovian	0.12	μVIS X-Ray Imaging Centre, University of Southampton, UK
<i>Cricosaurus araucanensis</i>	MLP 72-IV-7-1	Tithonian	0.448	Hospital Interzonal de Agudos de la Matanza "Dr. Diego Pairoissien" La Matanza, Argentina
<i>Cricosaurus schroederi</i>	MM Pa1	Valanginian	0.5	Leibniz Institute for Zoo and Wildlife Research, Berlin, Germany

2  
3

# Figure 1

Comparison of the palatal grooves in different thalattosuchian clades, skulls shown in palatal view.

(A) IVPP V 10098, Chinese teleosaurid; (B) NHMUK PV OR 32599, the early-diverging metriorhynchoid *Pelagosaurus typus*; (C) NHMUK PV R 3700, the metriorhynchid '*Metriorhynchus*' *brachyrhynchus*. Abbreviations: PG, palatal groove; SOG, suborbital groove.

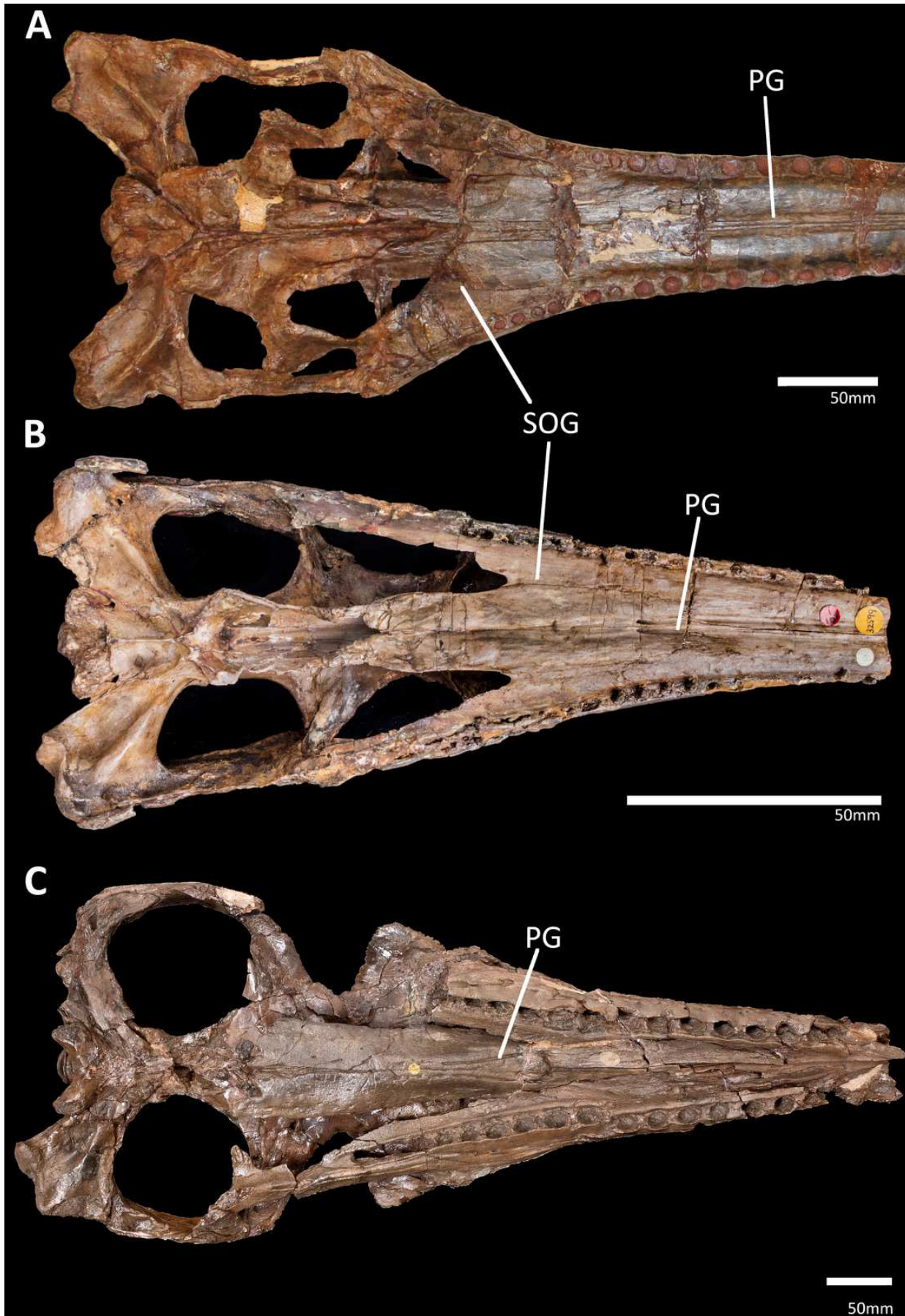


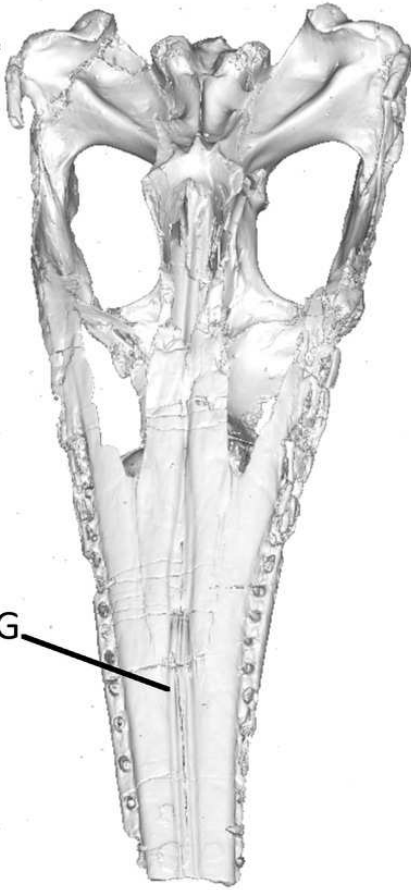


## Figure 2

Comparison between the thalattosuchian and extant crocodylians studied, CT reconstructions of the skulls shown in palatal view.

(A) NHMUK PV OR 32599, the early-diverging metriorhynchoid *Pelagosaurus typus*; (B) MLP 72-IV-7-1, the metriorhynchid *Cricosaurus araucanensis*; (C) UF herp 118998, the gavialid *Gavialis gangeticus*; (D) TMM M983, the alligatorid *Alligator mississippiensis*. Abbreviations: PG, palatal groove.

**A**  
20mm



**B**  
20mm



**C**  
20mm



**D**  
20mm

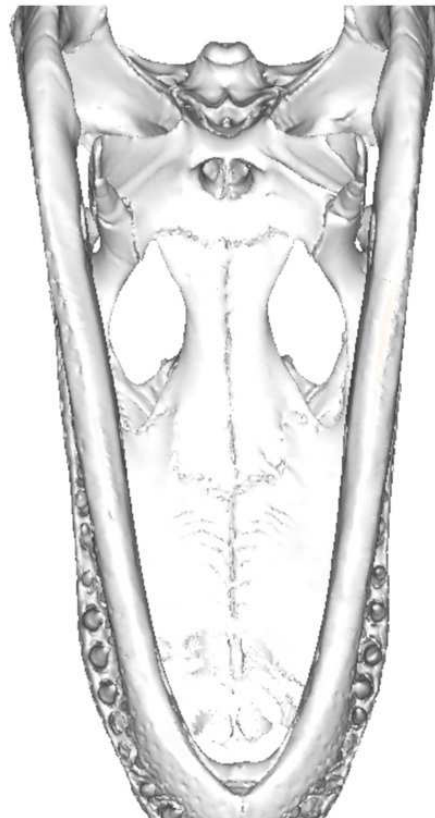


## Figure 3

Comparison of the extant crocodylians studied, CT reconstructions of the skulls shown in palatal view. Note, none of the extant crocodylians have palatal grooves.

(A) OUVC 10606, hatchling specimen of *Alligator mississippiensis*; (B) OUVC 9761, juvenile specimen of *Alligator mississippiensis*; (C) OUVC 11415, juvenile specimen of *Alligator mississippiensis*; (D) TMM M-983, juvenile specimen of *Alligator mississippiensis*; (E) USNM 211233, adult specimen of *Alligator mississippiensis*; (F) FMNH 73711, subadult specimen of *Caiman crocodilus*; (G) FMNH 59071, adult specimen of *Crocodylus acutus*; (H) MNB AB50.071, adult specimen of *Crocodylus rhombifer*; (I) TMM M-4980, adult specimen of *Crocodylus moreletii*; (J) OUVC 10899, juvenile specimen of *Crocodylus porosus*; (K) FMNH 98936, adult specimen of *Osteolaemus tetraspis*; (L) TMM M-6807, subadult specimen of *Crocodylus johnstoni*; (M) TMM M-3529, adult specimen of *Mecistops cataphractus*; (N) TMM M-5490, subadult specimen of *Gavialis gangeticus*; (O) UF herp 118998, adult specimen of *Gavialis gangeticus*; (P) TMM M-6342, subadult specimen of *Tomistoma schlegelii*; (Q) USNM 211322, adult specimen of *Tomistoma schlegelii*.

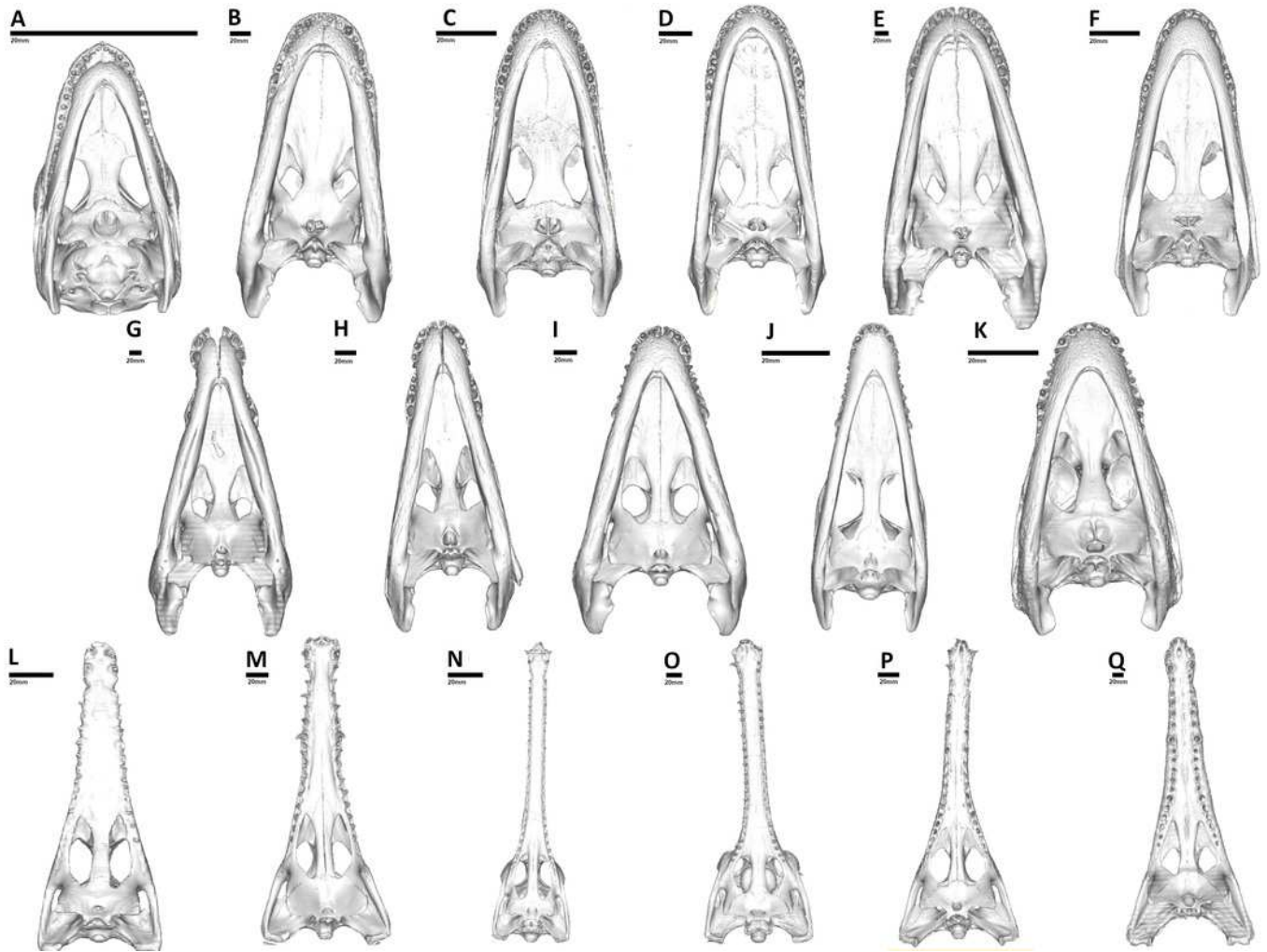


## Figure 4

The early-diverging teleosauroid *Plagiophthalmosuchus gracilirostris* (NHMUK PV OR 15500), from the early Toarcian of the UK.

(A) snout coronal view showing the position of the palatal canals. Three-dimensional reconstruction of the skull in (B) dorsal, and (C) lateral view, both showing the palatal canals in red and the CT slice of (A) shown in blue. Abbreviations: Alv, alveolus; DAC, dorsal alveolar canal; PC, palatal canal.

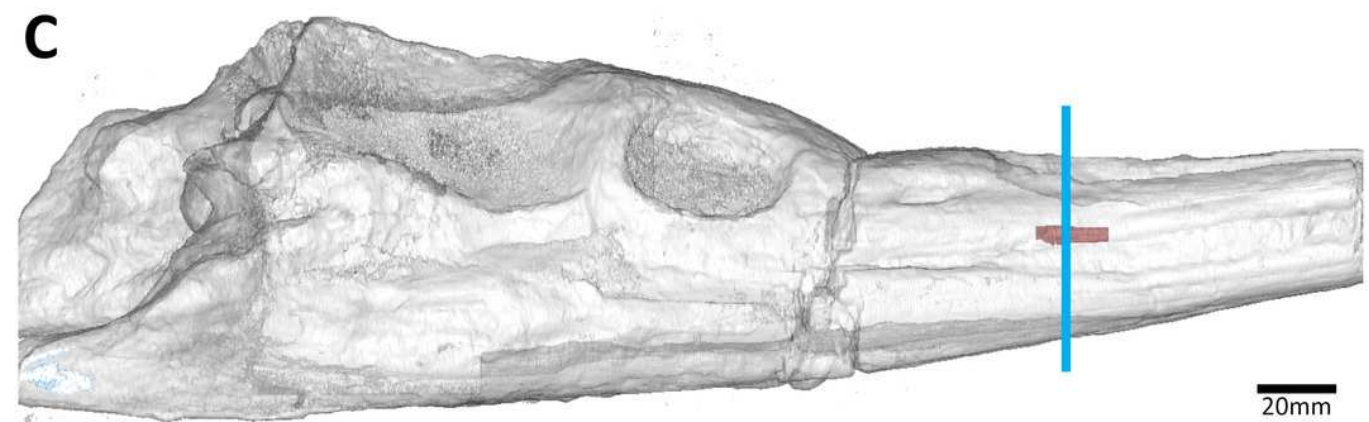
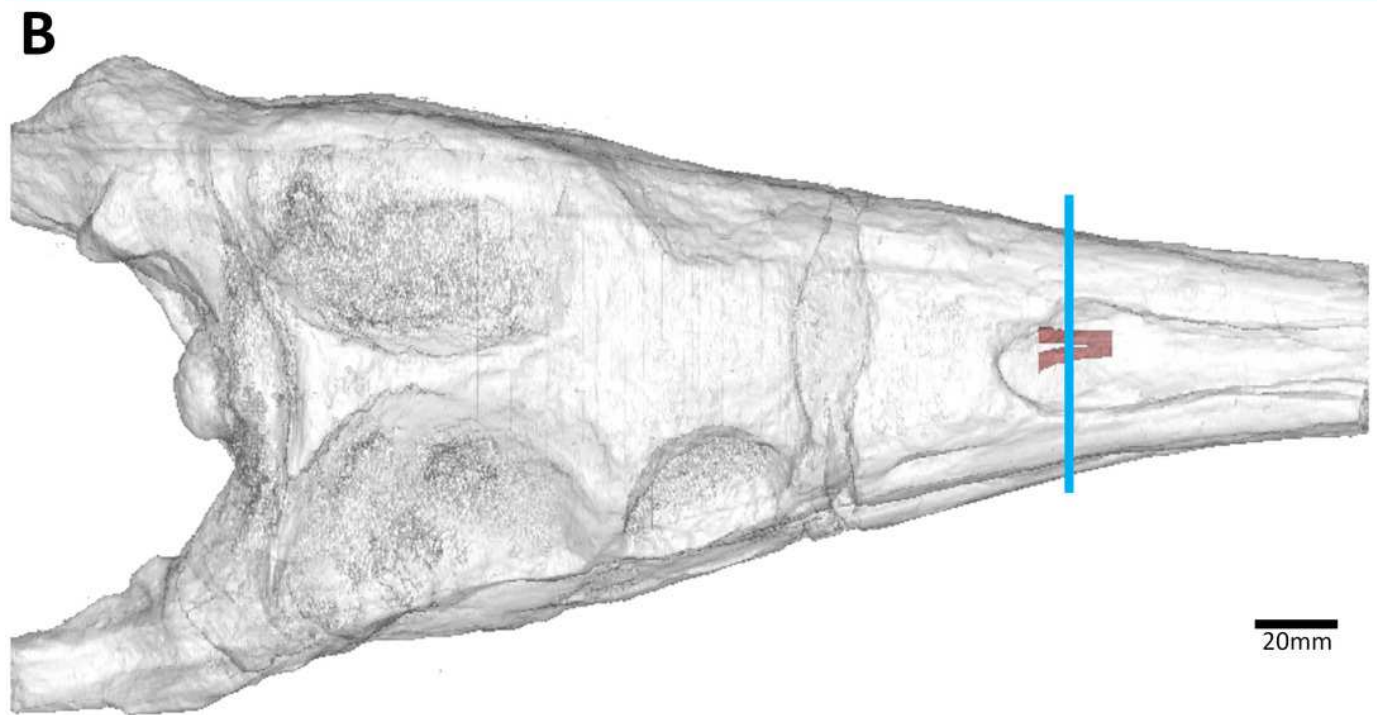
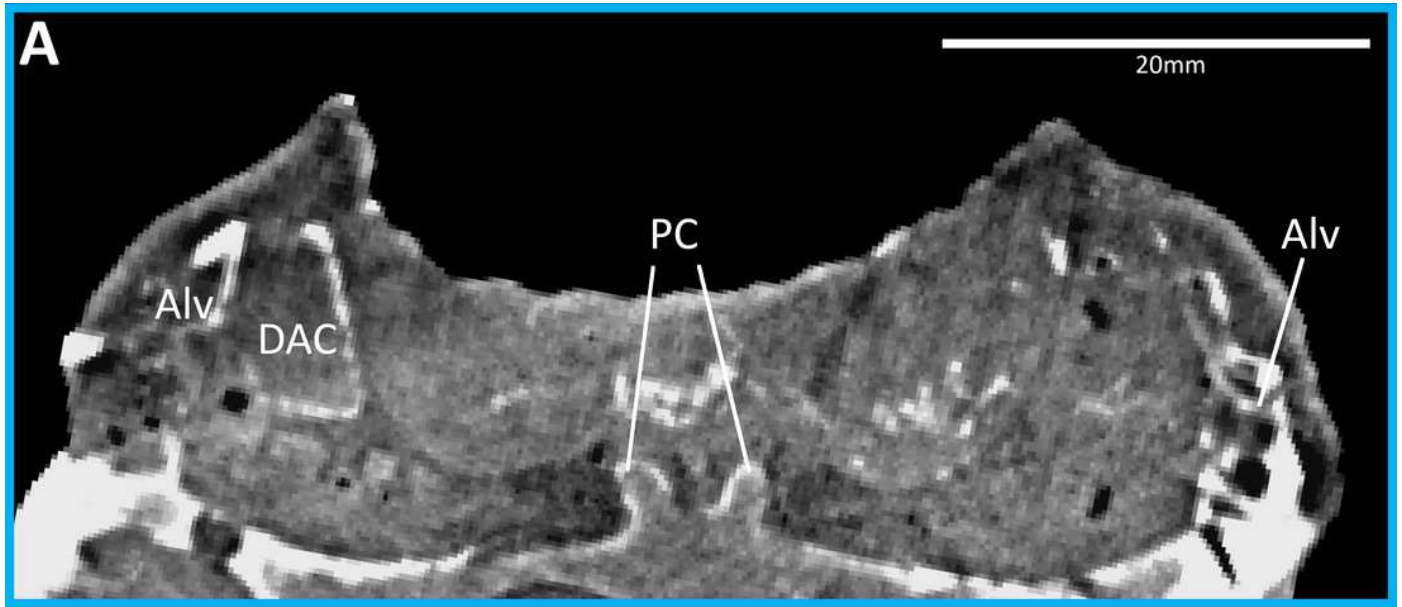


## Figure 5

The early-diverging metriorhynchoid *Pelagosaurus typus* (NHMUK PV OR 32599) referred specimen, early Toarcian of France.

(A) snout coronal view showing the position of the palatal canals. Three-dimensional reconstruction of the skull in (B) dorsal, and (C) lateral view, both showing the palatal canals in red and the CT slice of (A) shown in blue. Abbreviations: Alv, alveolus; DAC, dorsal alveolar canal; PC, palatal canal.

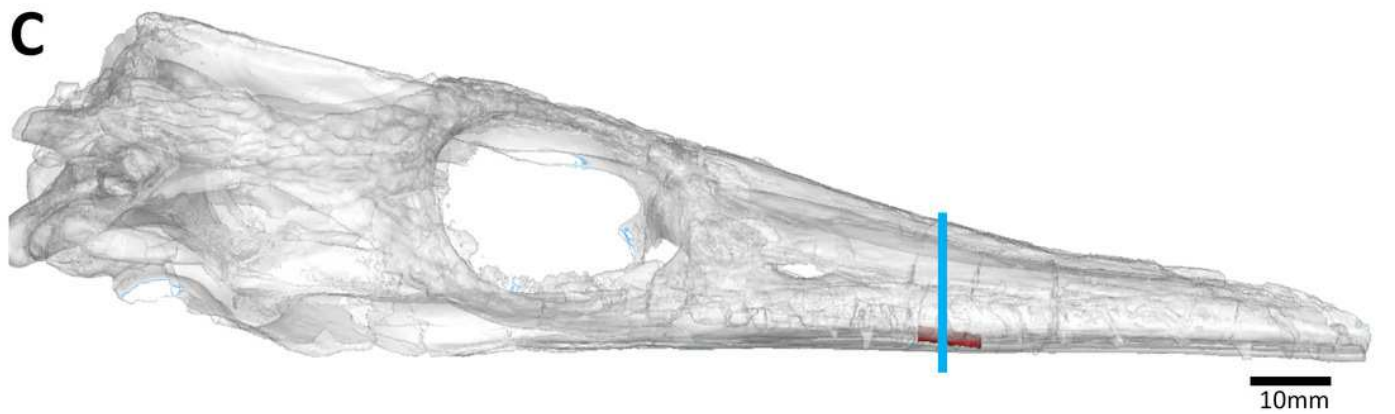
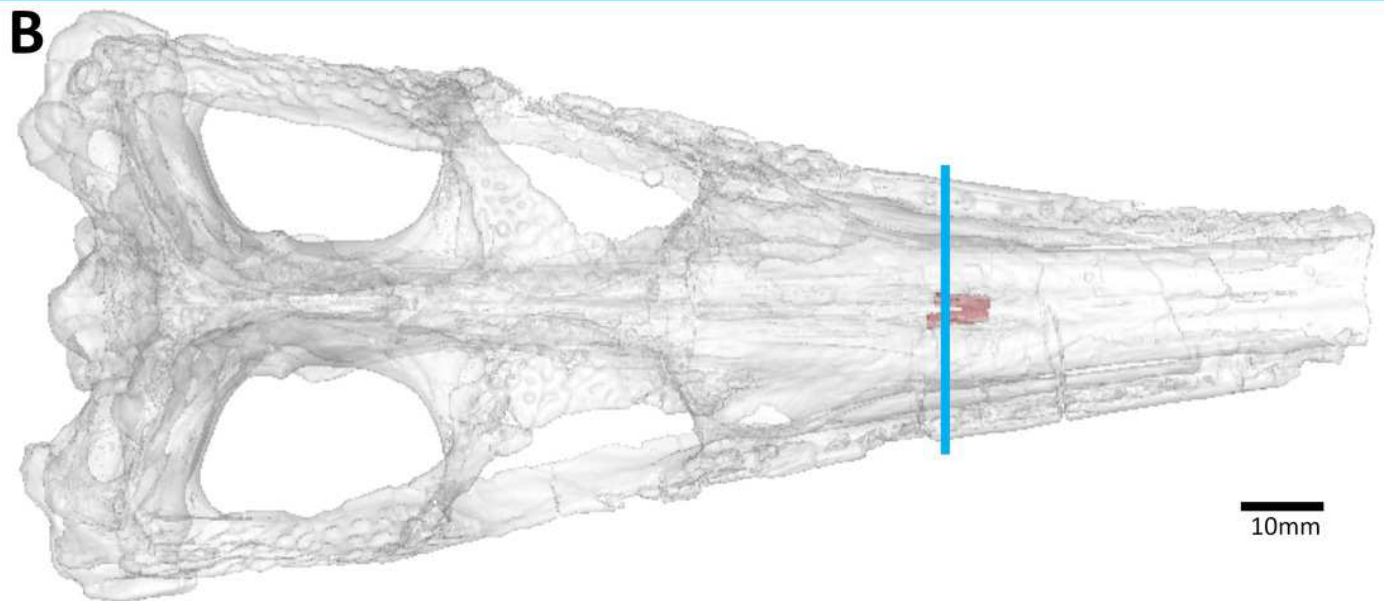
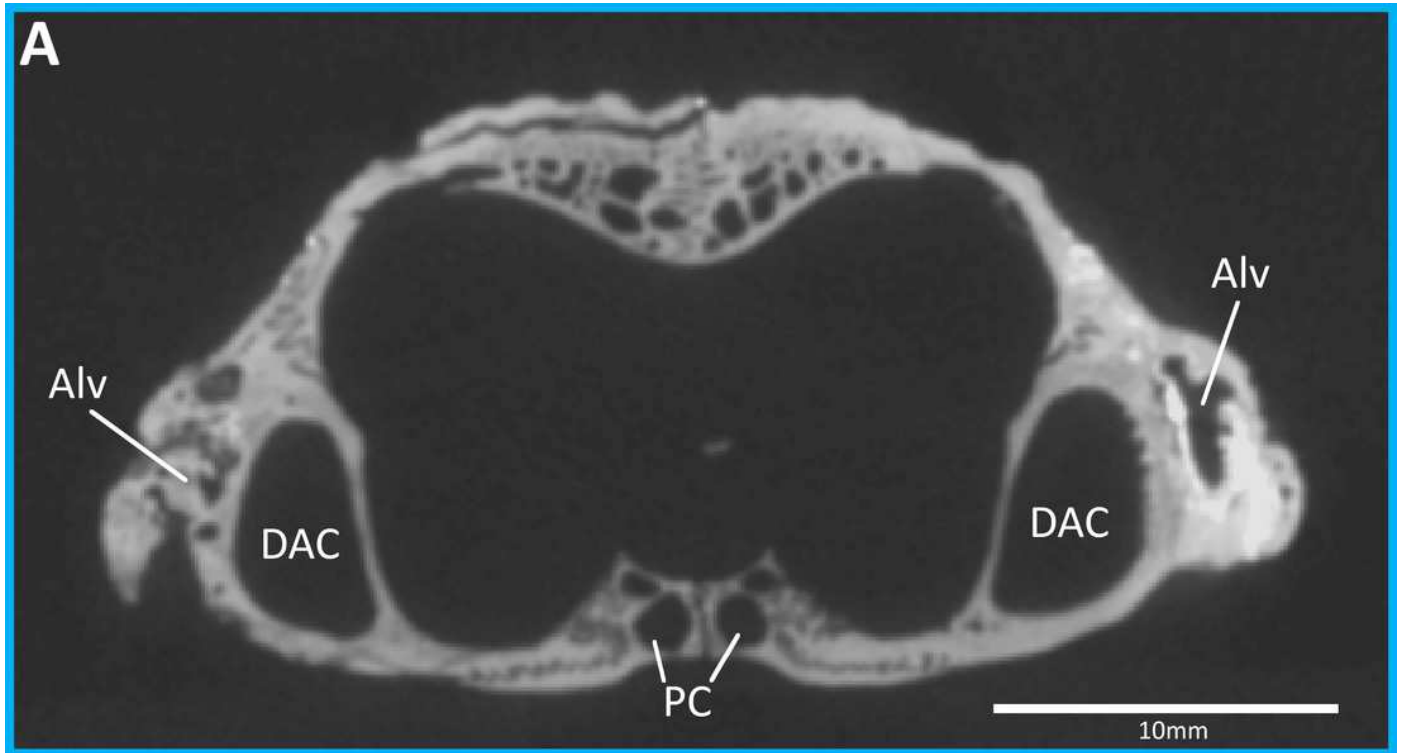
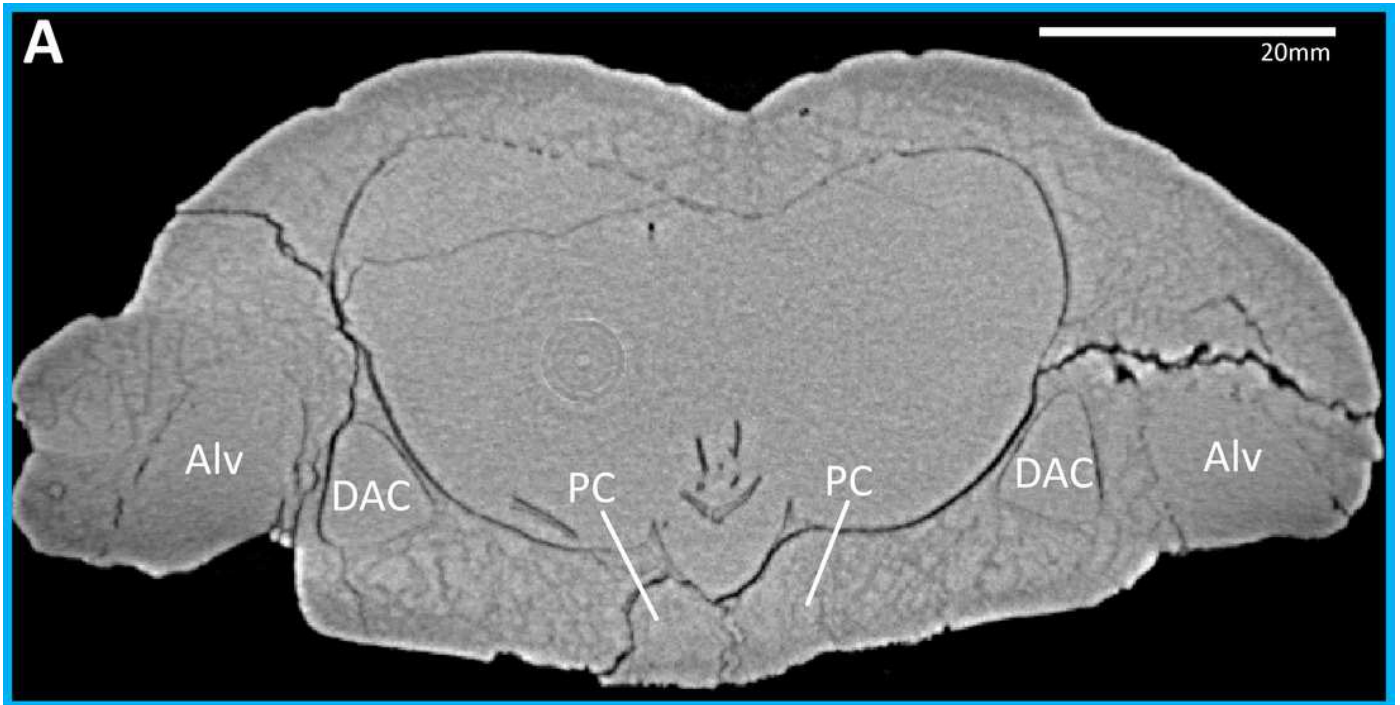




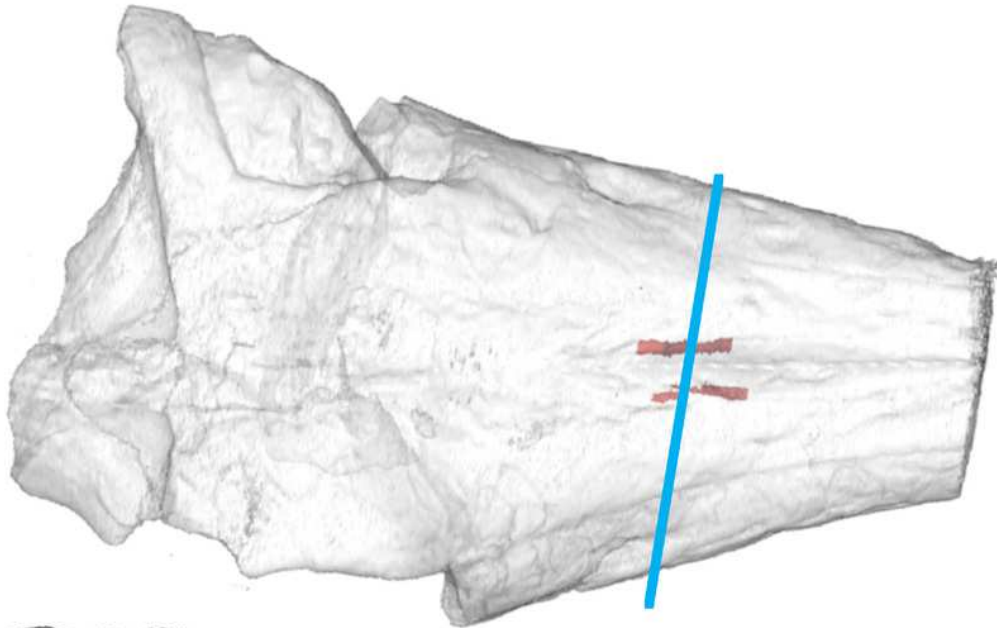
## Figure 6

The early-diverging metriorhynchoid *Eoneustes gaudryi* (NHMUK PV R 3263) holotype, Bathonian of France.

(A) snout coronal view showing the position of the palatal canals. Three-dimensional reconstruction of the skull in (B) dorsal, and (C) lateral view, both showing the palatal canals in red and the CT slice of (A) shown in blue. Abbreviations: Alv, alveolus; DAC, dorsal alveolar canal; PC, palatal canal.



**B**



**C**

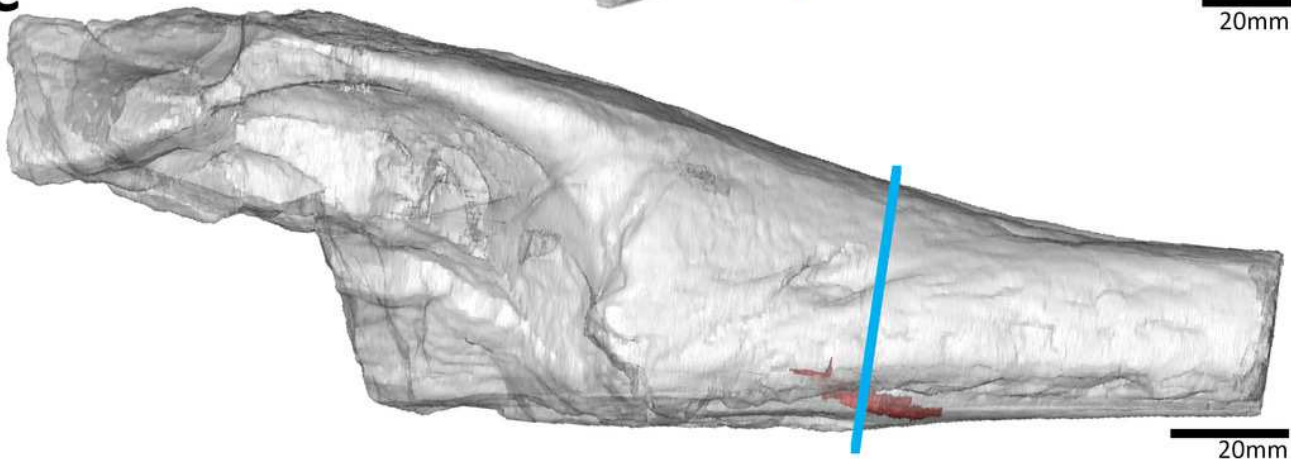


## Figure 7

The metriorhynchid *Thalattosuchus superciliosus* (NHMUK PV R 11999) referred specimen, middle Callovian of the UK.

(A) snout coronal view showing the position of the palatal canals. Three-dimensional reconstruction of the skull in (B) dorsal, and (C) lateral view, both showing the palatal canals in red and the CT slice of (A) shown in blue. Abbreviations: Alv, alveolus; DAC, dorsal alveolar canal; PC, palatal canal.

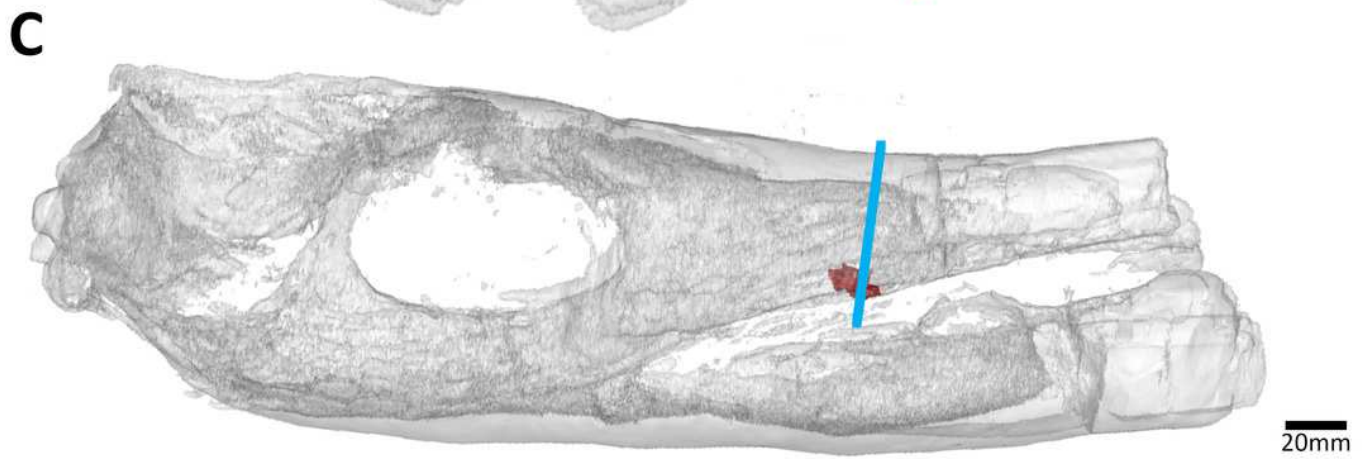
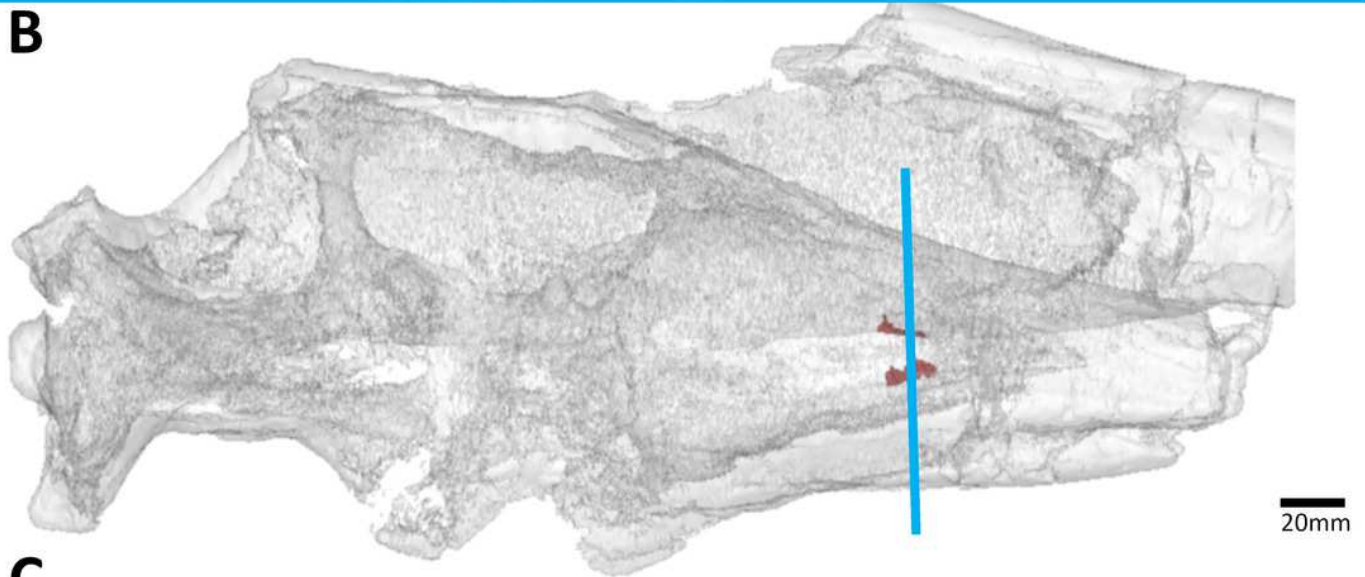
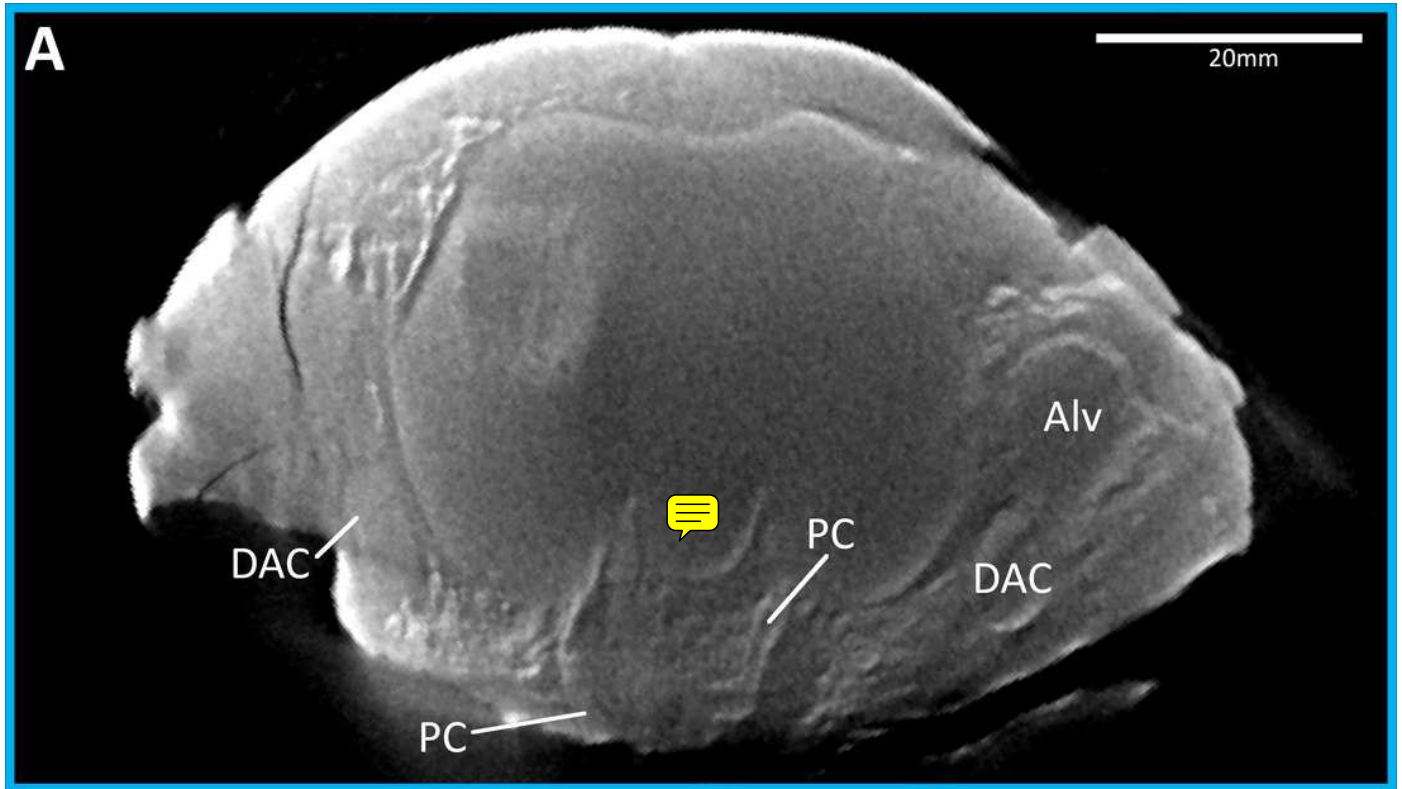
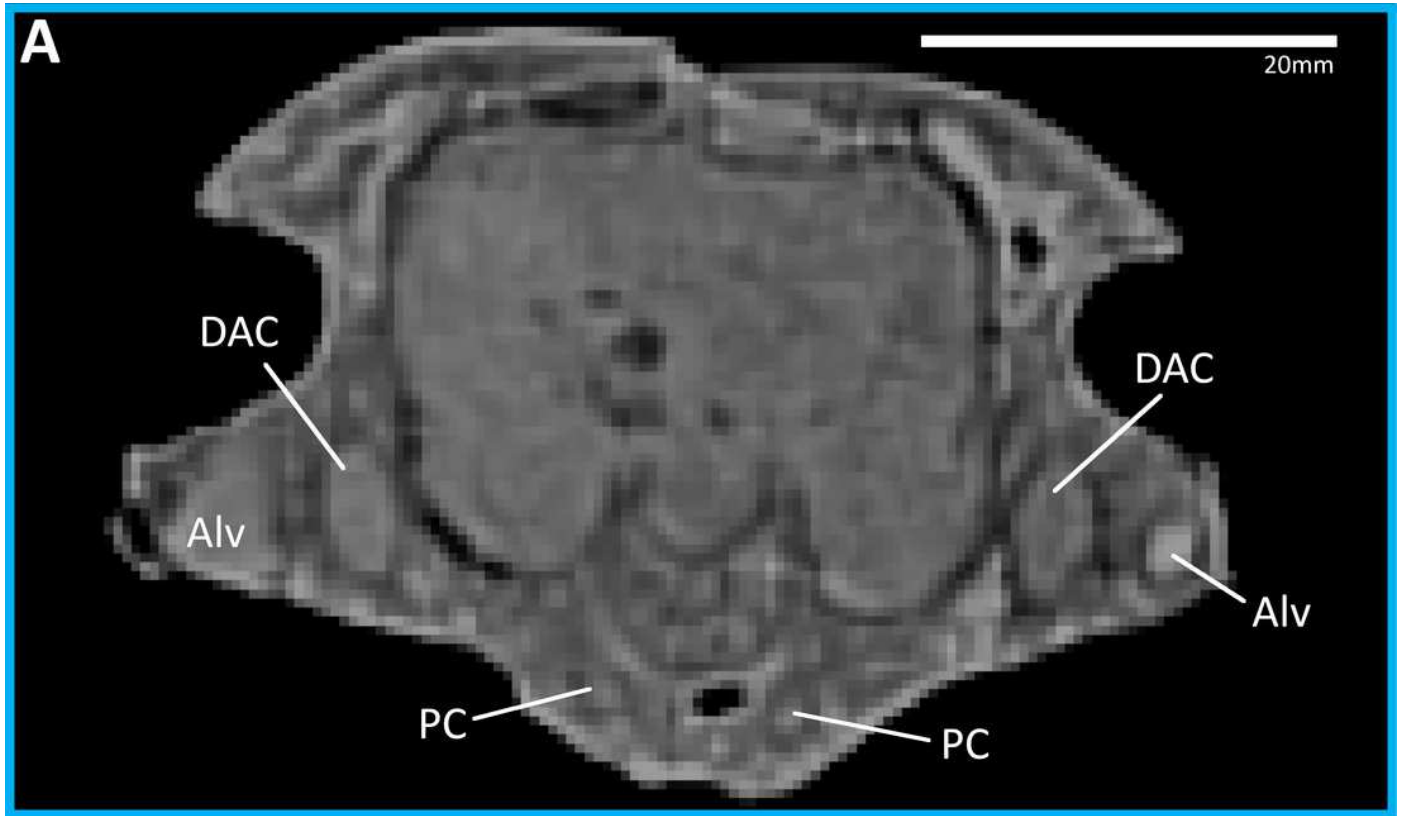


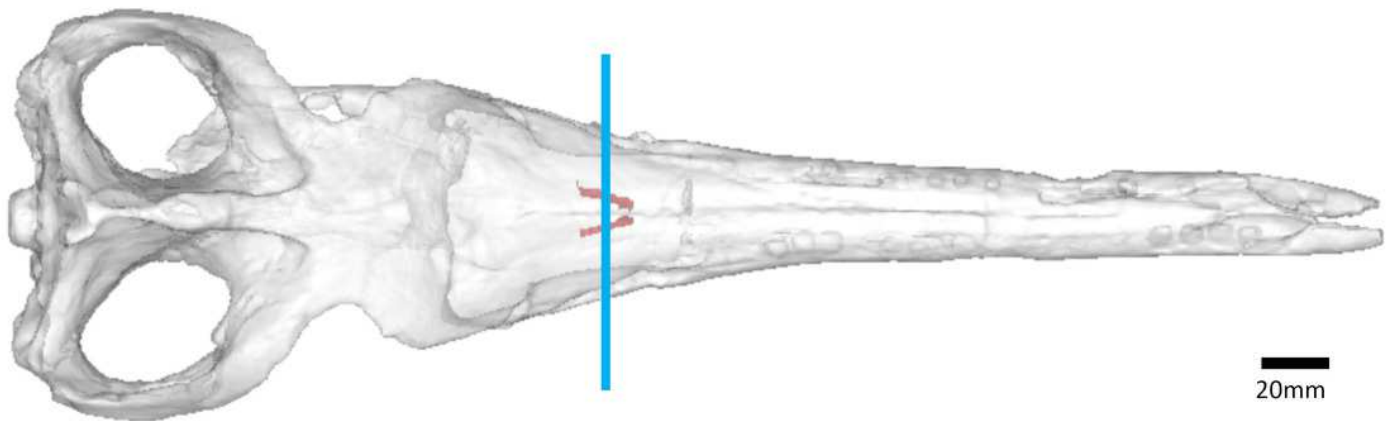
## Figure 8

The metriorhynchid *Cricosaurus araucanensis* (MLP 72-IV-7-1) holotype, Tithonian of Argentina.

(A) snout coronal view showing the position of the palatal canals. Three-dimensional reconstruction of the skull in (B) dorsal, and (C) lateral view, both showing the palatal canals in red and the CT slice of (A) shown in blue. Abbreviations: Alv, alveolus; DAC, dorsal alveolar canal; PC, palatal canal.



**B**



**C**

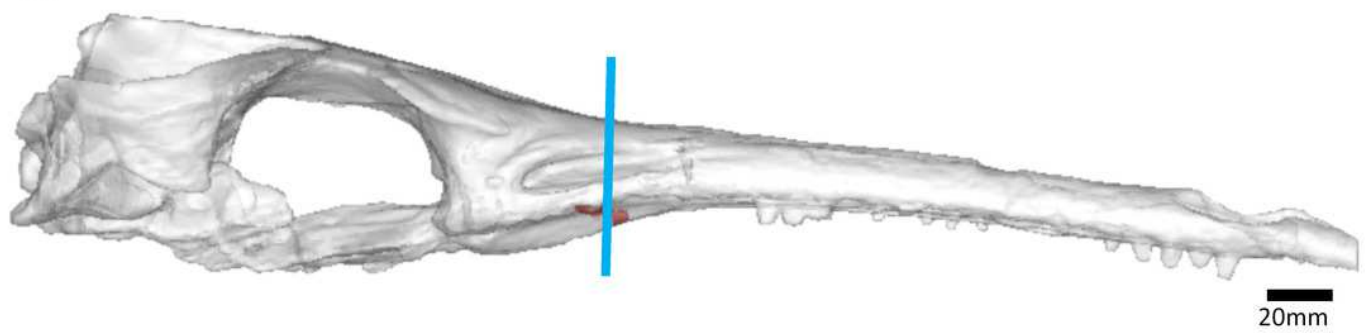
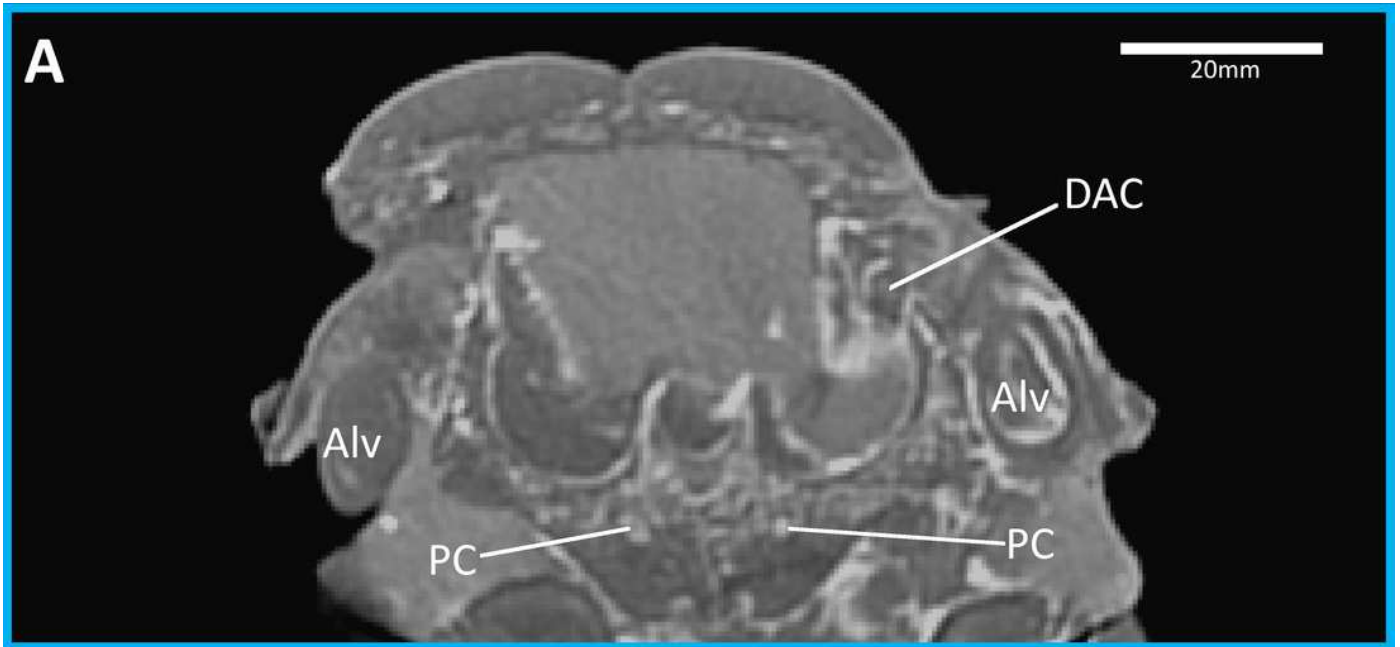


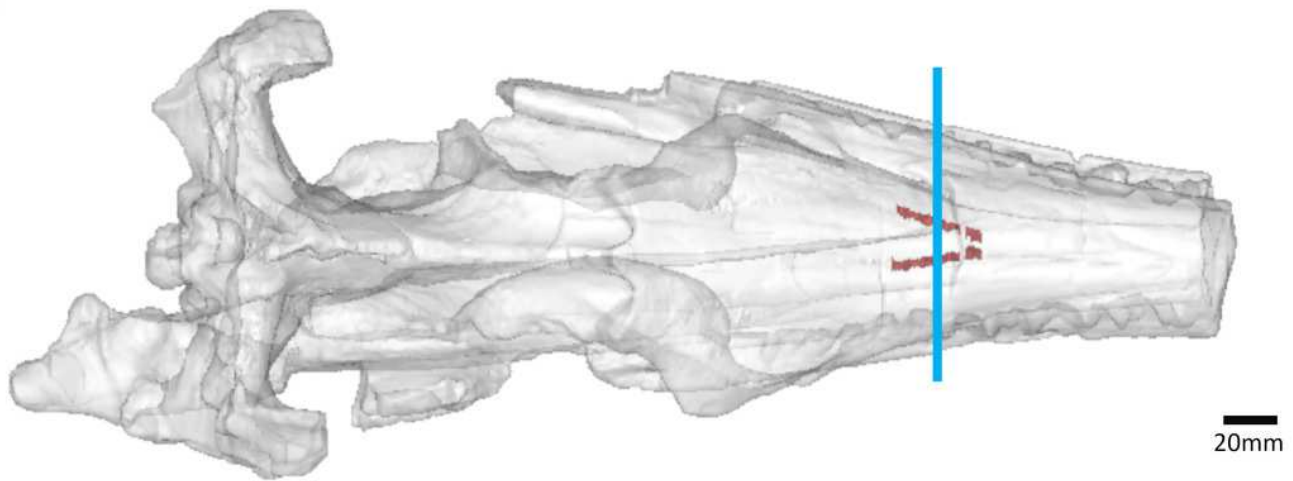
## Figure 9

The metriorhynchid *Cricosaurus schroederi* (MM Pa1), from the early Valanginian of Germany.

(A) snout coronal view showing the position of the palatal canals. Three-dimensional reconstruction of the skull in (B) dorsal, and (C) lateral view, both showing the palatal canals in red and the CT slice of (A) shown in blue. Abbreviations: Alv, alveolus; DAC, dorsal alveolar canal; PC, palatal canal.



**B**



**C**

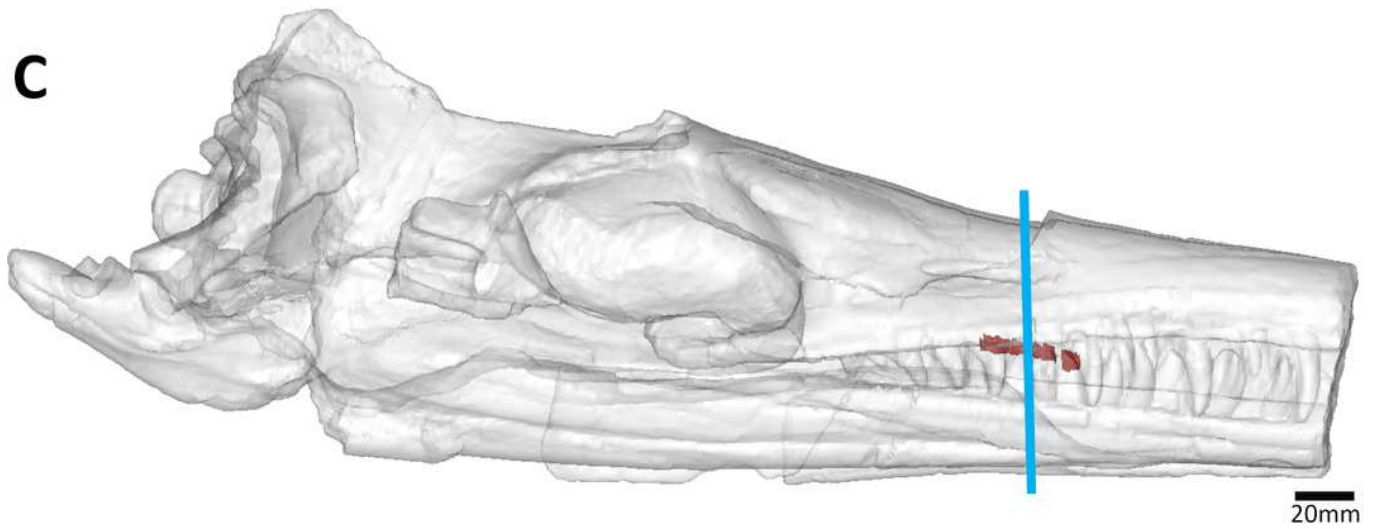




## Figure 10

The extant gavialid *Gavialis gangeticus* (UF-herp-118998).

(A) snout coronal view showing the lack of palatal canals. Three-dimensional reconstruction of the skull in (B) dorsal, and (C) lateral view, both showing the palatal canals in red and the CT slice of (A) shown in blue. Abbreviations: Ant, antorbital pneumatic sinus; Alv, alveolus; DAC, dorsal alveolar canal; Nas, nasal cavity.

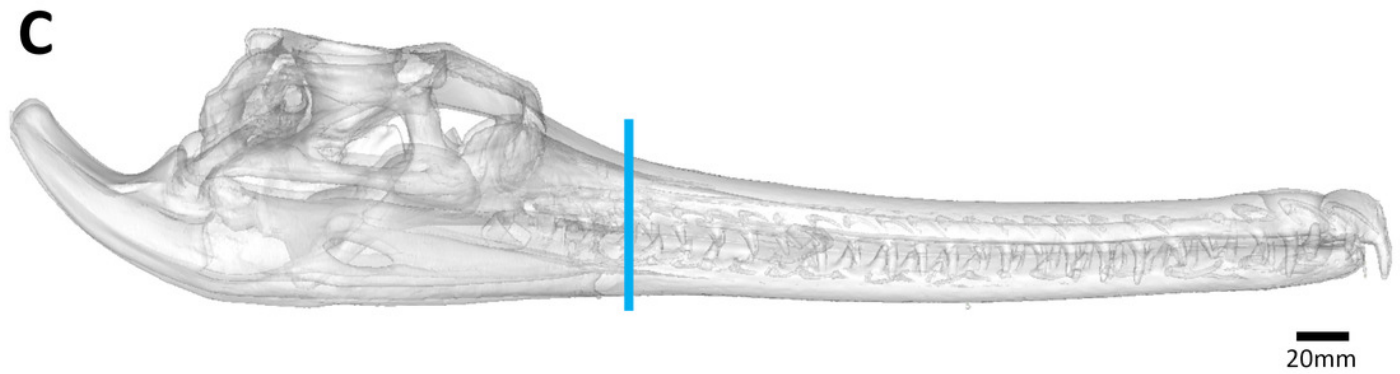
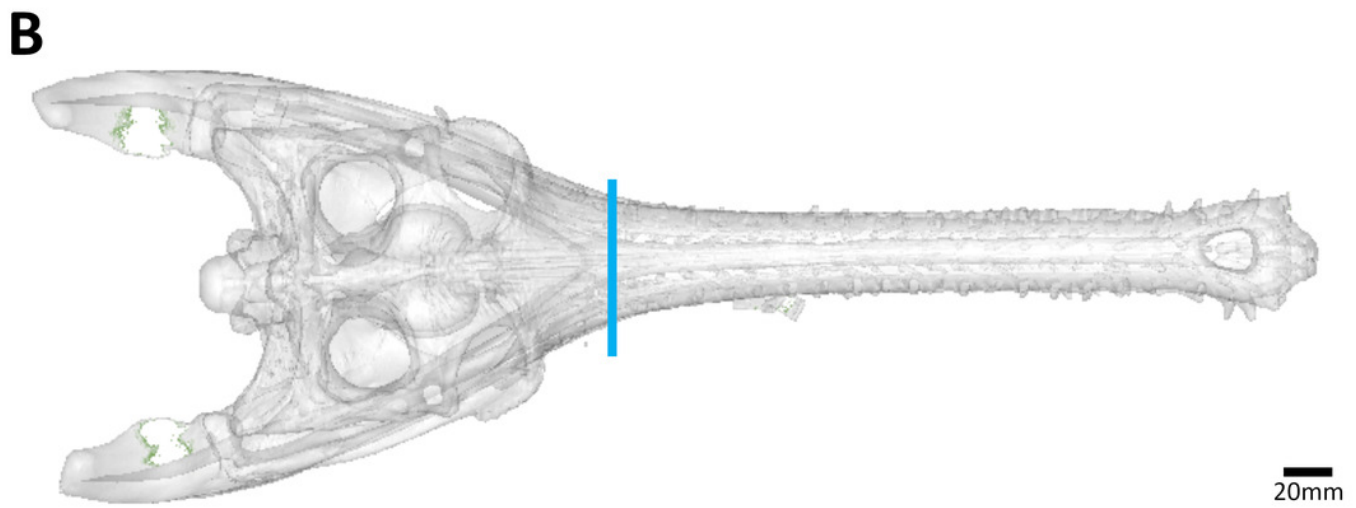
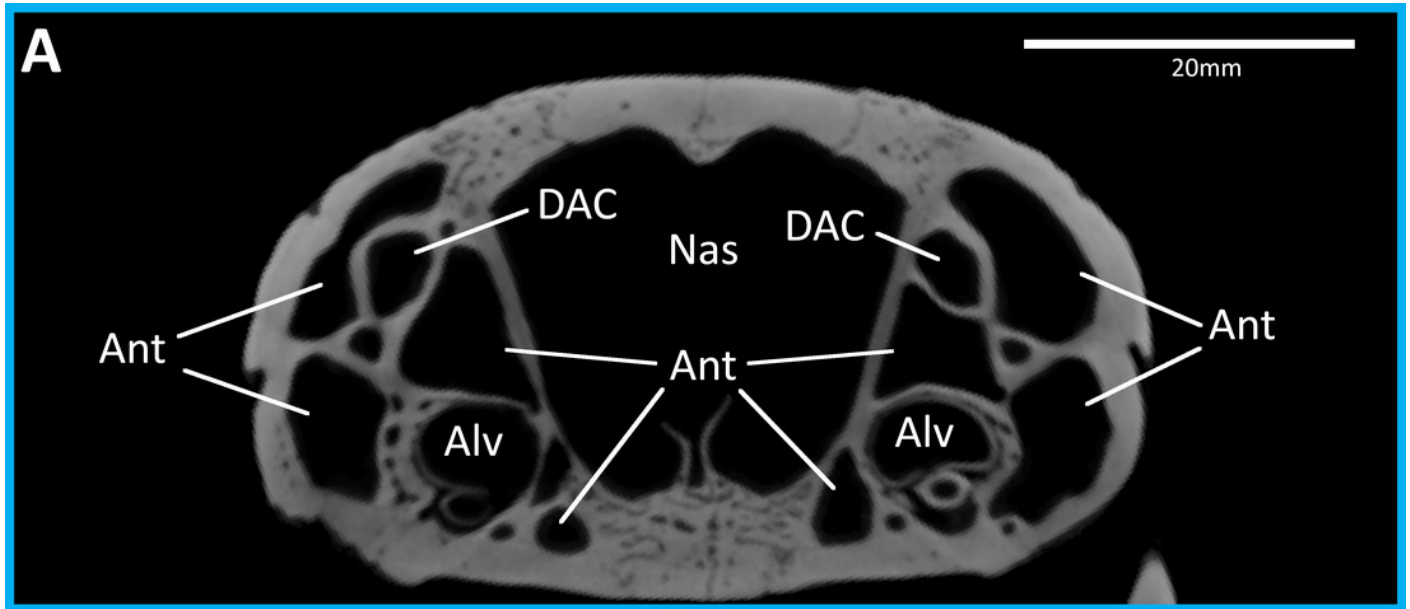


## Figure 11

The extant alligatorid *Alligator mississippiensis* (USNM 211233).

(A) snout coronal view showing the lack of palatal canals. Three-dimensional reconstruction of the skull in (B) dorsal, and (C) lateral view, both showing the palatal canals in red and the CT slice of (A) shown in blue. Abbreviations: Ant, antorbital pneumatic sinus; Alv, alveolus; Nas, nasal cavity.

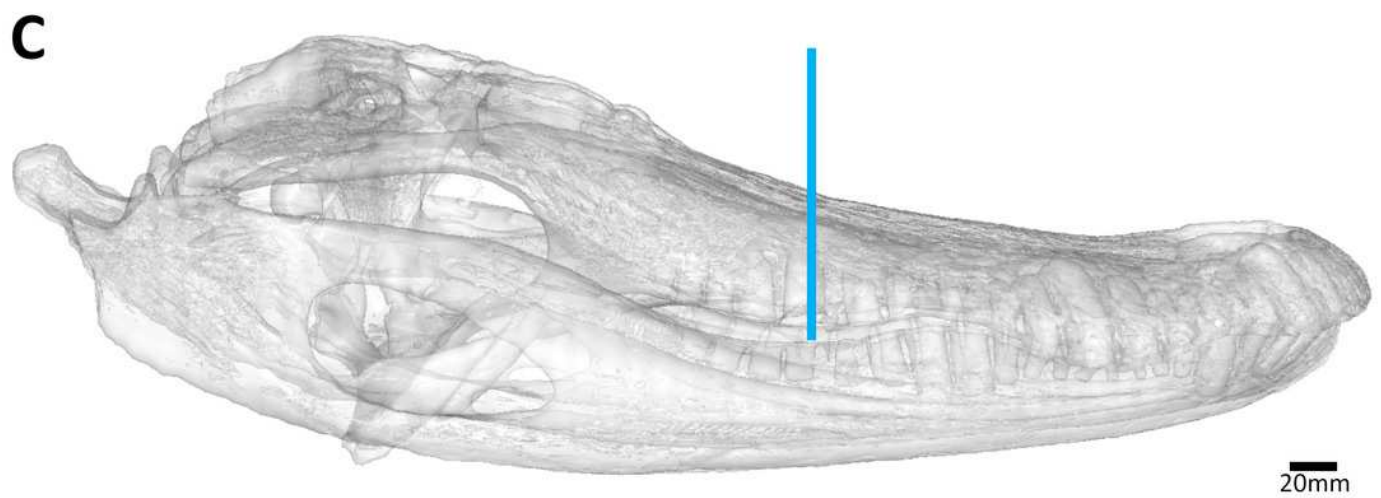
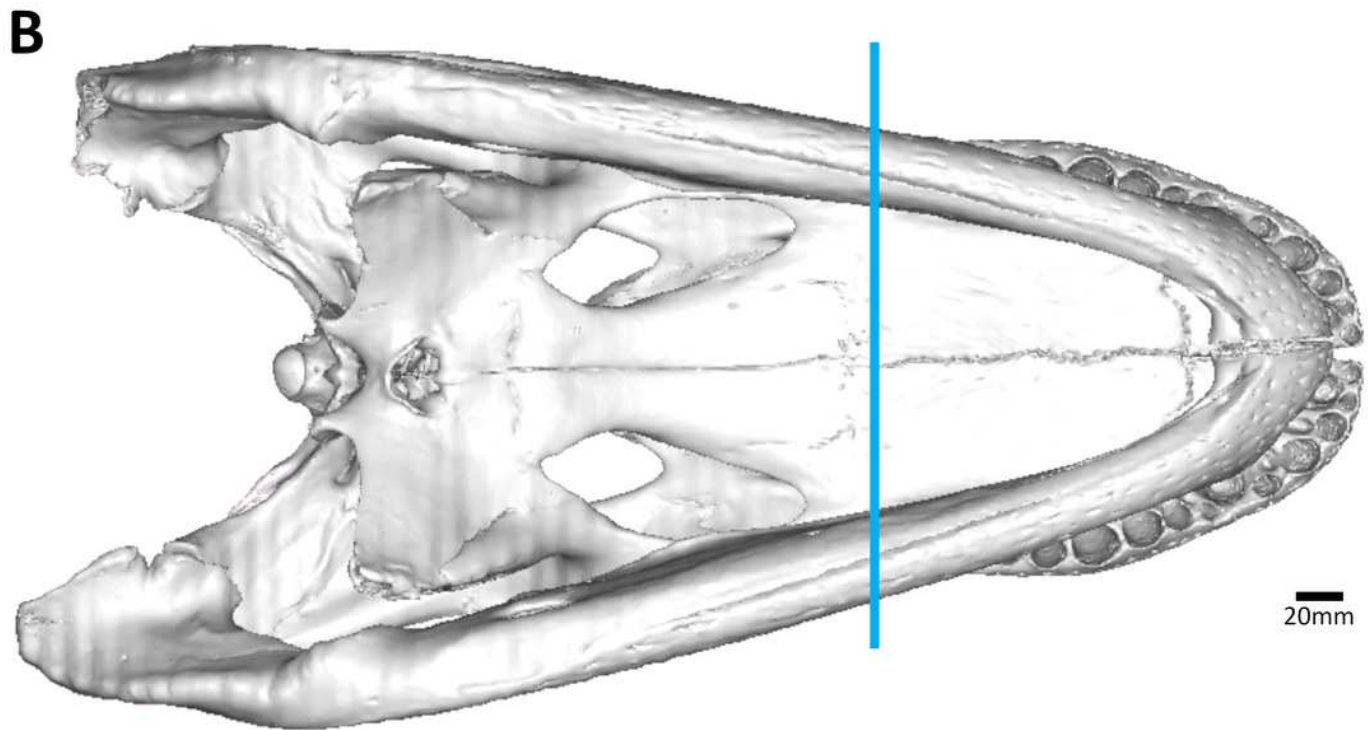
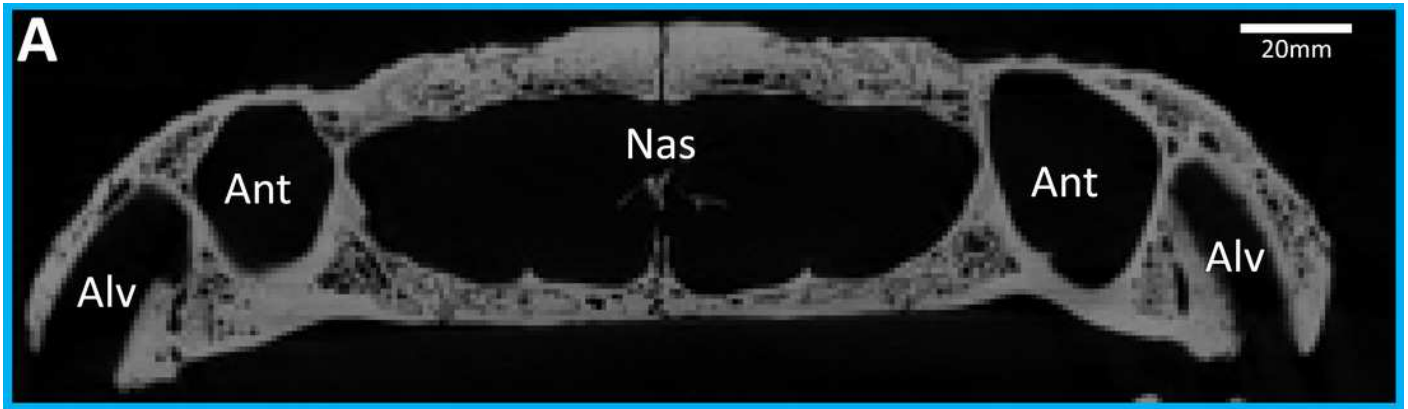


## Figure 12

The extant humpback whale (*Megaptera novaeangliae*).

(A) skull showing the palate, due to size the skull it is shown at an angle; (B) a close-up on the right palatal groove. Abbreviations: PG, palatal groove.



## Figure 13

Comparison of the palatal grooves in different extant odontocete cetaceans, skulls shown in palatal view.

(A) Cuvier's beaked whale (*Ziphius cavirostris*) NMS 2020.9.26; (B) killer whale (*Orcinus orca*) NMS Z.2015.179. Abbreviations: PG, palatal groove.



## Figure 14

Comparison of the palatal grooves in different extant pinnipeds, skulls shown in palatal view.

(A) the Antarctic fur seal (*Arctocephalus gazella*) NMS 2007.91.10; (B) the Leopard seal (*Hydrurga leptonyx*) NMS 1822.240.T29; (C) the Harbour seal (*Phoca vitulina*) NMS 1996.99.13. (A) is an otariid, while (B) and (C) are phocids. Abbreviations: PG, palatal groove.

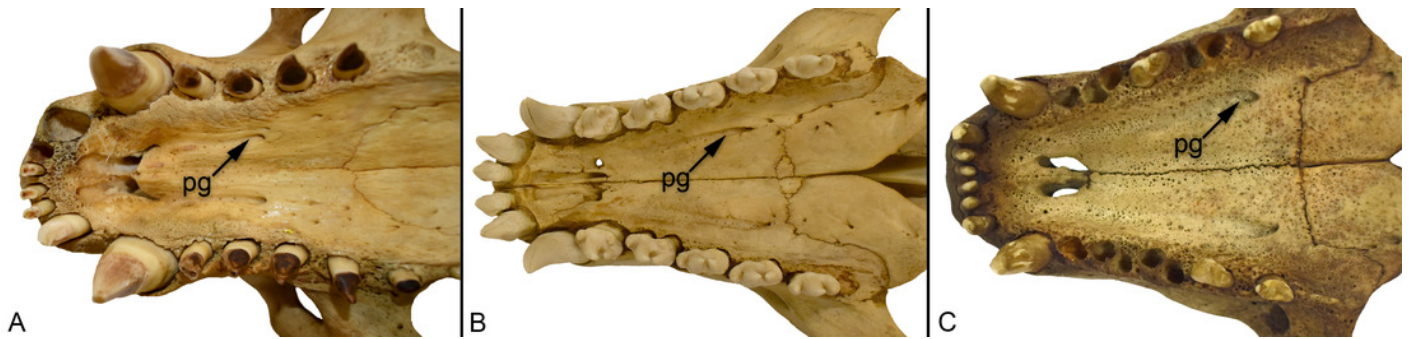


## Figure 15

The extant alligatorid *Alligator mississippiensis* (OUVC 9757) in dorsal view.

Cephalic vasculature with the medial nasal artery/vein shown in yellow and the palatine artery/vein and palatal plexus shown in red, (A) with the transparent skull, and (B) just the vasculature. Abbreviations: a+vMedNas, medial nasal artery and vein; a+vPal, palatine artery and vein; a+vPPlex, arterial and venous palatal plexus.



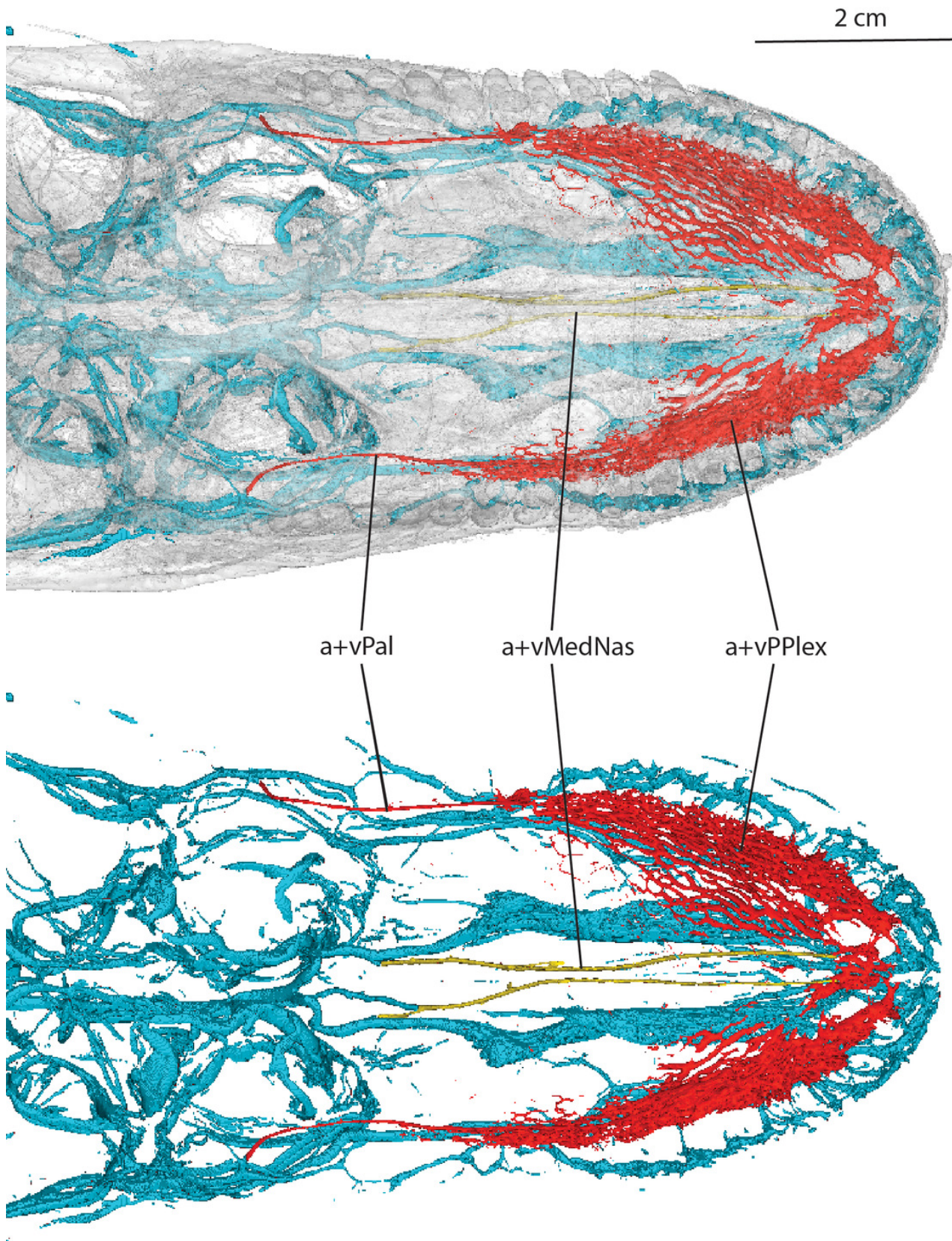


## Figure 16

The extant alligatorid *Alligator mississippiensis* (OUVC 9757) in lateral view.

Cephalic vasculature with the medial nasal artery/vein shown in yellow and the palatine artery/vein and palatal plexus shown in red, (A) with the transparent skull, and (B) just the vasculature. Abbreviations: a+vMedNas, medial nasal artery and vein; a+vPal, palatine artery and vein; a+vPPlex, arterial and venous palatal plexus.

